

# Osteology and chondrocranial morphology of *Gastrophryne carolinensis* (Anura: Microhylidae), with a review of the osteological diversity of New World microhylids

Linda Trueb<sup>1,2</sup>, Raul Diaz<sup>2</sup> and David C. Blackburn<sup>1,3</sup>

<sup>1</sup> Biodiversity Institute, Division of Herpetology, 1345 Jayhawk Blvd., University of Kansas, Lawrence, Kansas 66045-7561, USA. E-mail: trueb@ku.edu.

<sup>2</sup> Stowers Institute for Medical Research, 1000 E. 50th Street, Kansas City, Missouri 64110, and The University of Kansas Medical Center, Anatomy and Cell Biology, Kansas City, Missouri 66160, USA. E-mail: lissamphibia@gmail.com.

<sup>3</sup> Present address: Section of Herpetology, Department of Vertebrate Zoology & Anthropology, California Academy of Sciences, 55 Music Concourse Drive, Golden Gate Park, San Francisco, California 94118, USA. E-mail: blackburn@gmail.com.

## Abstract

**Osteology and chondrocranial morphology of *Gastrophryne carolinensis* (Anura: Microhylidae), with a review of the osteological diversity of New World microhylids.**

Microhylidae is a large, cosmopolitan anuran family. Recent molecular analyses have demonstrated the monophyly of the family—a conclusion that is supported by the larval morphology, coupled with the unique mode of tongue protrusion in adults, and a suite of osteological and myological characters seemingly associated with this innovation in feeding. Despite this functional constraint, osteological diversity probably exceeds that of any other anuran family, and this diversity is especially evident in the New World microhylids that comprise two clades, Gastrophryninae and Otophryninae. To facilitate comparisons among these clades, we describe the larval chondrocranium, skeletal development, and adult osteology of *Gastrophryne carolinensis*. We provide a phylogenetic context for these comparisons through a novel phylogenetic analysis of 45 microhylid genera based on data for one mitochondrial and three nuclear loci from previously published studies. Nearly all relationships within the monophyletic Gastrophryninae are resolved with robust support. Based on these results, we found that the larval chondrocrania of gastrophrynines share morphological features that distinguish them from *Otophryne* and other anurans. Among the adults, all gastrophrynines show evidence of an anterior shift of the jaws that is correlated with specializations in the otic region, and with the alignment of the planum antorbitale, the cartilage wall separating the nasal capsule from the orbits. The

---

Received 17 May 2011.  
Accepted 5 September 2011.  
Distributed December 2011.

larval infrarostral and the adult mandibles lack a typical anuran mandibular symphysis, and the mentomeckelian bone of the adult is modified with a special process. The most variable part of the skull is the palate in which a neopalatine usually is absent and the vomer may be single or divided. The posteromedial processes of the hyoids of gastrophrynines tend to be elaborated, and some taxa bear a peculiar transverse slit in the posterior part of the hyoid corpus. The anterior zonal elements of the pectoral girdle are reduced or absent, and the posterior parts enlarged and shifted posteriorly. Most taxa have eight presacral vertebrae; depending on the taxon the last presacral is amphicoelous or procoelous.

**Keywords:** Adult osteology, Gastrophryinae, larval chondrocranium, osteological diversity, phylogeny, skeletogenesis.

### Resumo

**Osteologia e morfologia do condrocânio de *Gastrophryne carolinensis* (Anura: Microhylidae), com uma revisão da diversidade osteológica dos Microhylidae do Novo Mundo.** A família Microhylidae é muito diversificada e cosmopolita. Análises moleculares recentes demonstraram seu monofiletismo—uma conclusão sustentada pela morfologia larval, ao lado do modo único de protrusão da língua nos adultos e de um conjunto de características osteológicas e miológicas aparentemente associadas à essa inovação na alimentação. Apesar dessa restrição funcional, a diversidade osteológica provavelmente excede à de qualquer outra família de anuros, e essa diversidade é especialmente evidente nos Microhylidae do Novo Mundo de dois clados, Gastrophryinae e Otophryinae. Para facilitar as comparações entre esses clados, descrevemos aqui o condrocânio larval, o desenvolvimento do esqueleto e a osteologia do adulto de *Gastrophryne carolinensis*. Fornecemos um contexto filogenético para essas comparações por meio de uma nova análise filogenética de 45 gêneros de Microhylidae baseada em dados de um locus mitocondrial e três loci nucleares obtidos em estudos prévios publicados. Quase todas as relações dentro do grupo monofilético Gastrophryinae são robustamente suportadas. Com base nesses resultados, concluímos que os condrocânios das larvas dos Gastrophryinae compartilham características morfológicas que os distingue de *Otophryne* e de outros anuros. Entre os adultos, todos os Gastrophryinae mostram evidências de uma mudança na parte anterior das maxilas relacionada a especializações na região ótica e ao alinhamento do *planum antorbitale*, a parede de cartilagem que separa a cápsula nasal das órbitas. Os infra-rostrais das larvas e as mandíbulas dos adultos são desprovidos de uma sínfise mandibular típica dos anuros, e o osso mentomeckeliano do adulto é modificado com um processo especial. A porção mais variável do crânio é o palato, no qual o neopalatino geralmente está ausente e o vômer pode ser simples ou dividido. Os processos póstero-mediais dos hióides dos Gastrophryinae tendem a ser elaborados, e alguns táxons possuem uma fenda transversal peculiar na porção posterior do corpo do hióide. Os elementos zonais anteriores da cintura escapular são reduzidos ou ausentes, e as porções posteriores, aumentadas e deslocadas posteriormente. A maioria dos táxons possui oito vértebras pré-sacrais; dependendo do táxon, a última vértebra pré-sacral é anficélica ou procélica.

**Palavras-chave:** Condrocânio larval, diversidade osteológica, esqueletogênese, filogenia, Gastrophryinae, osteologia.

## Introduction

The anuran family Microhylidae (sensu Frost *et al.* 2006) is a species-rich clade and among the most taxonomically diverse of all amphibians (11 subfamilies; nearly 70 genera, >490 species; AmphibiaWeb 2011). Microhylids are distributed globally throughout tropical and temperate regions and the clade includes taxa with a wide and diverse range of morphologies, ecologies, and life histories (Duellman and Trueb 1994, Wells, 2007). Among anurans, microhylids are notable for both unusual morphologies and a highly specialized mode of feeding by which prey are captured with a tongue that is protruded by hydrostatic elongation (Meyers *et al.* 2004). Many microhylid species share broadly similar bauplans characterized by a globular body shape and a short, pointed head. There is, however, substantial morphological variation among microhylids, including features that are rare or absent in other anuran clades (e.g., Noble and Parker 1926, Parker 1934, Carvalho 1948, 1954, Zweifel, 1972, 1986, de Sá and Trueb 1991, Wu 1994, Wild, 1995). Many of these distinctive anatomical features pertain to the bony skeleton, specifically the skull, hyoid, pectoral girdle, and the phalanges (Parker 1934, Carvalho 1948, 1954, Zweifel 1962, 1971, 1985, 2000, Zweifel and Allison, 1982, Zweifel and Parker 1989, Wild 1995, Lehr and Trueb 2007); soft tissue of the palate (Parker 1934, Carvalho 1948); and larval morphologies (e.g., Donnelly *et al.* 1990, Lavilla and Langone 1995, Haas 2001, 2003). There is a significant body of literature dealing with the cranial anatomy of microhylids that has been largely overlooked. This includes the contributions of de Villiers (1930, 1934), Ramaswami (1932a, b, 1940), and Jurgens (1971).

Recent molecular estimates of phylogenetic relationships have resulted in new insights into microhylid phylogeny; genera such as *Breviceps* and *Callulina*, formerly included with microhylids, now are thought to be more closely related to the monotypic family Hemisotidae (and thus part of the Afrobatrachia, sensu Frost

*et al.* 2006) and the Hyperoliidae and Arthroleptidae (Darst and Cannatella 2004, van der Meijden *et al.* 2004, 2007, Frost *et al.* 2006). Although this phylogenetic perspective provides a context for understanding the evolution of morphological diversity in this rich clade, there are few anatomical studies of microhylids that provide the necessary data to describe and interpret the systematic, ontogenetic, and functional significance of the observed variation.

As a group, New World microhylids are morphologically diverse and recent phylogenies (e.g., Frost *et al.* 2006) suggest there may be a high degree of homoplasy in morphological characters. Recent taxonomic revisions based on the results of molecular phylogenetic studies (e.g., Frost *et al.* 2006) recognize two clades of extant microhylids that occur in North and South America, as well as an assortment of genera of uncertain phylogenetic affinity. Otophryinae is restricted to the three species of *Otophryne*, which are of note for their highly unusual tadpole morphology (Wassersug and Pyburn 1987). The other clade is the subfamily Gastrophryinae, which contains 65 species in 18 genera (AmphibiaWeb 2011). Within this latter clade, *Chiasmocleis* is the most speciose genus with 25 species; other gastrophryine genera contain between one and thirteen species. Last, there is a handful of microhylid genera restricted to South America that has not been included in a large-scale analysis of microhylid phylogeny. These genera have low species diversity and include *Adelastes*, *Altigius*, *Arcovomer*, *Hyophryne*, *Melanophryne*, *Myersiella*, *Stereocyclops*, *Synapturanus*, and *Syncope*. Although there are many brief treatments of skeletal morphology of American microhylids (Parker 1881, Carvalho 1948, 1954, Walker, 1973, Walker and Duellman 1974, Zweifel 1986, da Silva and Meinhardt 1999), there are few comprehensive studies. To date, there are thorough descriptions of the skeletal morphology in only four genera—*Elachistocleis* (Lavilla *et al.* 2003), the monotypic *Hamptophryne* (de Sá and Trueb 1991), *Melanophryne*, and *Nelsonophryne* (Lehr and Trueb

2007). In addition, Donnelly *et al.* (1990), Haas (2001, 2003), Pugener *et al.* (2003) and Vera Candiotti (2006, 2007) described and discussed morphological variation of larval characteristics for a number of microhylid genera. As a contribution to knowledge of skeletal morphology in American microhylids, we describe the adult osteology, ossification sequence, and chondrocranium of *Gastrophryne carolinensis*, a common species that occurs throughout much of the southeast United States. The chondrocranium and adult skeletal osteology are described first, and followed by an account of the ossification sequence. We then review the patterns of larval and adult morphological diversity in New World microhylids, and compare their morphology to that of African phrynomerines for which there are more osteological data and functional morphological observations.

## Materials and Methods

Morphological study is based on 40 larval and 8 adult specimens of *Gastrophryne carolinensis* (Holbrook, 1835) in the collection of the Division of Herpetology in the University of Kansas Natural History Museum and Biodiversity Institute (Appendix I). Larvae were staged in accordance with Gosner (1960) and span Stages 26–46. Skeletal preparations were made using the cleared-and-stained method following the protocols of Dingerkus and Uhler (1977) and Klymkowsky and Hanken (1991), with minor modifications; specimens at Gosner stages earlier than 33 stained poorly. Snout–vent length was measured prior to clearing and staining for all specimens for which this was feasible. Comparisons with other taxa are based on examination of skeletal preparations already existing in museum collections.

Terminology and format follow those of de Sá and Trueb (1991) and Lehr and Trueb (2007), with minor exceptions such as the identity of the manual digits for which we follow the terminology of Alberch and Gale (1985) and Fabrezi and Alberch (1996). Drawings were

prepared with the aid of a dissecting stereoscope and camera lucida.

A phylogenetic context is necessary for interpreting patterns of skeletal variation across the Microhylidae. Two recent studies provide estimates of phylogenetic relationships within the Microhylidae (Frost *et al.* 2006, van der Meijden *et al.* 2007) yet they contain markedly different taxon sampling. Of the 17 microhylid genera sampled in these studies, 14 were sampled only by Frost *et al.* (2006) and another 8 were sampled only by van der Meijden *et al.* (2007). Because of other recent phylogenetic analyses including microhylid taxa (Van Bocxlaer *et al.* 2006, Wollenberg *et al.* 2008), genetic data are also available for microhylid genera not included in the studies by Frost *et al.* (2006) and van der Meijden *et al.* (2007). Rather than base our morphological comparisons on these multiple phylogenies with different taxon sampling, we performed a new phylogenetic analysis that included available data for 45 genera (of the nearly 70 total genera) of microhylids (Appendix II). This analysis included all of the taxa sampled by Frost *et al.* (2006) and van der Meijden *et al.* (2007), with the exception of *Callulops slateri* from Frost *et al.* (2006) for which we could not satisfactorily align the available data to those for other taxa. We also included data for five additional genera (*Barygenys*, *Cophyla*, *Hylophorbus*, *Melanobatrachus*, *Metaphrynella*, and *Xenobatrachus*) from the studies by Van Bocxlaer *et al.* (2006) and Wollenberg *et al.* (2008). Because data for *Synapturanus* derive from specimens identified as *Synapturanus* sp. and *Synapturanus mirandaribeiroi*, we consider this as a composite taxon in our analysis (Appendix II). As outgroup to root the resulting phylogeny, we used the distantly related neobatrachian frog *Pyxicephalus* (Frost *et al.* 2006; Roelants *et al.* 2007). Our analysis included data for the four genetic loci sampled with greatest intensity by these studies: the mitochondrial locus containing 12S and 16S ribosomal RNA (and the intervening transfer RNA for Valine), and the nuclear loci recombination activating genes 1 and 2 (*RAG-1*

and *RAG-2*) and the gene for the enzyme tyrosinase (*TYR*). We generated a multiple sequence alignment for each locus using either default parameters in ClustalX (*RAG-1*, *RAG-2*, and *TYR*; Thompson *et al.* 1997) or MUSCLE (mitochondrial locus; Edgar 2004). We determined the best model of sequence evolution for each locus via calculation of the Akaike Information Criterion (AIC) in jModelTest (Posada 2008): mitochondrial – (GTR + I +  $\Gamma$  model,  $\ln L = -31873.30$ , AIC = 63982.61; vs. next best model GTR +  $\Gamma$ :  $\ln L = -31921.53$ , AIC = 64077.06); *RAG-1* – (GTR +  $\Gamma$ ,  $\ln L = -12299.77$ , AIC = 24833.54; vs. next best model GTR + I +  $\Gamma$ :  $\ln L = -12299.86$ , AIC = 24835.72); *RAG-2* – (HKY +  $\Gamma$ ,  $\ln L = -8382.70$ , AIC = 16991.40; vs. next best model GTR +  $\Gamma$ :  $\ln L = -8381.89$ , AIC = 16997.77); *TYR* – (HKY + I +  $\Gamma$  model,  $\ln L = -6200.13$ , AIC = 12628.26; vs. next best model GTR + I +  $\Gamma$ :  $\ln L = -6197.69$ , AIC = 12631.38). We estimated the phylogenetic relationships using a maximum likelihood analysis in GARLI-Partition Ver. 0.97 (Zwickl 2006); we partitioned the analysis by locus and applied the best-fit model of sequence evolution to each partition. As our best estimate of phylogenetic relationships, we used the ML phylogeny with the lowest  $-\ln$  likelihood score from 100 search replicates in GARLI; each search was terminated  $10 \times 10^5$  generations after the last topological improvement. We estimated support using 100 nonparametric bootstrap replicates in GARLI, using the same model of sequence evolution and search specifications, but with only one search replicate per bootstrap replicate.

## Results

### Chondrocranium

*Early larval chondrocranium – Gosner Stage 34.*—By any measure, the chondrocranium of the Stage-34 larva looks peculiar (Figure 1). Owing to the small size and delicacy of the specimen, and substandard staining, it is impossible to

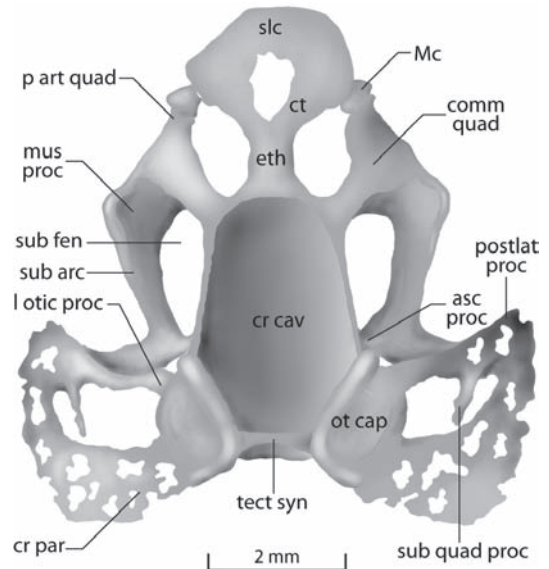


**Figure 1.** Chondrocranium of Stage-33 larva of *Gastrophryne carolinensis* in dorsal aspect. Note the fusion of the superior labial cartilage with the cornua trabeculae, the presence of a posterolateral process on the palatoquadrate that is united with the crista parotica. Abbreviations: asc proc = ascending process; comm quad = commissura quadratocranialis anterior; cr cav = cranial cavity; cr par = crista parotica; ct = cornu trabeculae; eth = ethmoid plate; l otic proc = larval otic process; Mc = Meckel's cartilage; mus proc = muscular process; ot cap = otic capsule; p art quad = pars articularis quadrati; postlat proc = posterolateral process; slc = superior labial cartilage; sub fen = subocular fenestra; sub quad proc = subotic quadrate process; tect syn = tectum synoticum.

determine the disposition of the basicranial fenestra and foramina. In dorsal/ventral aspects, the chondrocranium is triangular in shape. At its greatest width across the otic region, the chondrocranium is 150% wider than it is at the level of the muscular processes. The rostral part of the chondrocranium (i.e., that part anterior to the anterior margin of the frontoparietal fontanelle) comprises 43% of the total length of the larval skull. The apex of each muscular

process lies posterior to the quadratocranial commissure at approximately the level of the anterior margin of the frontoparietal fontanelle (= posterior margin of ethmoid plate). The distance between the pair of apices is 119% that between the lateral margins of the otic capsules. The chondrocranium bears broad, fenestrate plates of cartilage extending laterally from the well-formed otic capsules posteriorly, and a prominent “spoonbill” composed of the planum internasale, cornu trabeculae, and suprarostrale (= superior labial cartilage), anteriorly. The frontoparietal fontanelle is undivided. The fontanelle is widest at the anterior margin of the otic capsule, and is approximately 1.5× longer than its greatest width. Its lateral margins are formed by the taenia tecti marginalis and the anterior border defined by the ethmoid plate; the tectum synoticum, which forms a slender bridge between the otic capsules, forms the posterior border of the fontanelle.

The ethmoid plate is moderately long. Anteriorly, a pair of short, flat cornua trabeculae diverges laterally from the planum. The cornua are fused to a broad cartilaginous plate formed by the fusion of the suprarostrale cartilages to form the superior labial cartilage. The suprarostrale projects anteroventrally and is ventrally concave; thus, in dorsal view, it completely obscures underlying elements of the lower jaw (Meckel’s and infrarostrale cartilages). The larval mandible is composed of the pair of Meckel’s cartilage posteriorly and a keyhole-shaped infrarostrale (inferior labial) cartilage anteriorly.

The ventromedial margin of the palatoquadrate is slightly arcuate and together with the lateral margin of the braincase, describes a teardrop or seed-shaped subocular fenestra from a dorsal view. The lateral margin of the palatoquadrate is angular; the long axis of the element posterior to the muscular process diverges from the posterior region of the braincase at approximately a 30° angle. The muscular process is laterally convex, and directed at a slight dorsolateral angle; the apex of the process lies approximately at the level of the anterior margin of the frontoparietal

fontanelle. The commissura quadratocranialis is long, slender, and distally expanded at its union with the palatoquadrate anterior to the muscular process. Anteriorly, a well-defined articular process provides a point of articulation for Meckel’s cartilage. Posteriorly, the palatoquadrate bifurcates. A slender medial process, the processus ascendens, connects the palatoquadrate to the lateral wall of the braincase at a point dorsolateral to the primary carotid foramen. The posterolateral process, the larval otic process, is broad and straplike, and extends laterally to the fenestrate larval crista parotica, where it folds back toward the skull in a dorsomedial direction to fuse with the anterior margin of the otic capsule. At the point of flexion of the otic process and its union with the fenestrate larval cartilage, the subotic quadrate process, an irregular-shaped spicule of cartilage, projects posteriorly into the large fenestra in the middle of the fenestrate cartilage. It should be noted that the crista parotica is limited to the posterolateral margin of the otic capsule.

*Late larval chondrocranium – Gosner Stage 41.*—The chondrocranium is significantly altered in appearance by Stage 41 (Figure 2A–C), being rectangular, rather than triangular, in overall shape. At its greatest width across the otic region, the skull is only marginally (109%) wider than it is at the level of the muscular processes. The rostral portion of the chondrocranium forward of the anterior margin of the frontoparietal fontanelle comprises 43% of the total length of the larval skull, as it did in the younger larva. However, the configuration of the anterior palatoquadrate is greatly changed. The apex of each muscular process is lateral to the quadratocranial commissure and anterior to the level of the frontoparietal fontanelle. The distance between the pair of apices is 160% that between the lateral margins of the otic capsules. Thus, by comparison with the Stage-34 larvae, the anterior palatoquadrate has become greatly elaborated anterolaterally—a process that significantly modifies the overall shape and appearance of the developing skull.

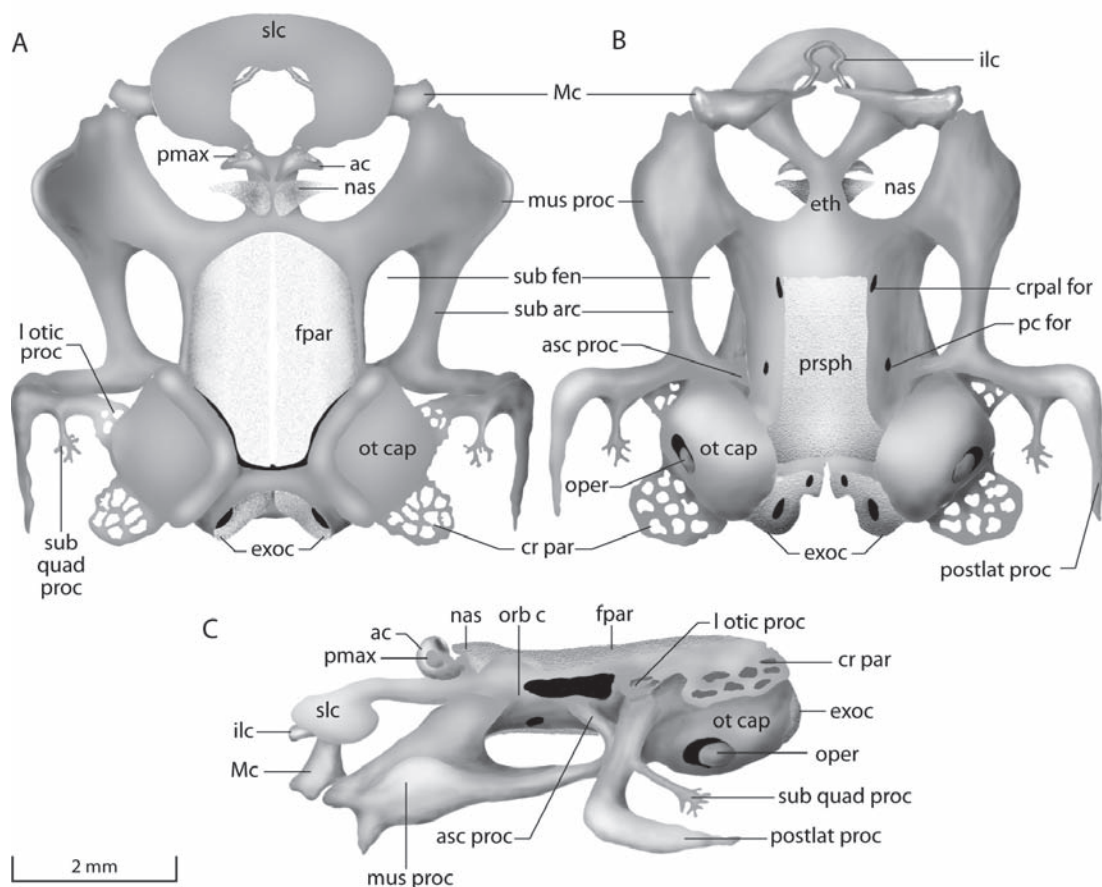


**Figure 2.** Chondrocranium of Stage-41 larva of *Gastrophryne carolinensis* in dorsal (A), ventral (B), and lateral (C) aspects. Abbreviations same as in Figure 1 with the following additions: ac = alary cartilage; crpal for = craniopalatal foramen; exoc = exoccipital; ilc = inferior labial cartilage; fpar = frontoparietal; nas = nasal; orb c = orbital cartilage; oper = operculum; pc for = primary carotid foramen; pmax = premaxilla; prsph = parasphenoid.

Another obvious change is the difference in the relative proportions of the fenestrate cartilage associated with the otic capsule and palatoquadrate to the overall size of the chondrocranium; it seems that the extent of the fenestrate cartilage is much reduced relative to the rest of the chondrocranium. A larval crista parotica is isolated from the palatoquadrate cartilages and associated only with the posterolateral margin of the otic capsule. The posterolateral fenestrate cartilage associated with

the posterolateral and larval otic processes of the palatoquadrate has become transformed into a single, large, posterior process. The subotic quadrate process lies medial to the posterolateral process and persists in the Stage-41 larva as a short, tree-like process projecting posteriorly from the larval otic process into the space between the otic capsule and posterior process of the palatoquadrate.

Frontoparietal bones roof the frontoparietal fontanelle (Figure 2A), and the parasphenoid

bridges the prootic and sphenethmoid cartilages ventrally (Figure 2B). The exoccipitals have begun to form the ventral part of the foramen magnum. The nasals are apparent dorsal to the ethmoid plate between the developing nasal cartilages and the anteriorly adjacent premaxillae. The suprarostrals are markedly broader in the Stage-41 larvae than in the Stage-34 larvae and forms a broad cartilaginous ring that, in dorsal view, mostly obscures the lower jaw cartilages.

The orbital cartilage composes the lateral wall of the braincase (Figure 2C), and its dorsal margin forms the taenia tecti marginalis of the frontoparietal fontanelle. The orbital cartilage is continuous with the tectum synoticum posteriorly and anteriorly with the ethmoid plate. The lateral wall of the chondrocranium is pierced by a large foramen, which presumably represents a single, common opening for components of Cranial Nerves II–VII (Cannatella 1999). The braincase is pierced by two pair of foramina adjacent to the lateral margin of the developing parasphenoid—the foramen craniopalatinum is located anteriorly, whereas the foramen caroticum primarium lies posterior, medial to the otic process of the palatoquadrate (de Sá and Trueb 1991).

The large, ovoid otic capsules are nearly one-third the length of the chondrocranium. Laterally, the fenestra ovalis lies below the posterior portion of the larval crista parotica and is approximately one fourth of the length of the otic capsule. A cartilaginous operculum lies within and covers nearly half of the fenestra ovalis.

Meckel's cartilages are robust, especially in comparison to the delicate infrarostral cartilage (Figure 2B). The base of the triangular Meckel's cartilage is broad at its lateral articulation with the palatoquadrate; the cartilage tapers to its anteromedial, hinge-like articulation with the infrarostral. The infrarostrals are fused medially to form a thin keyhole-shaped cartilage that projects anterodorsally. In Stage-34 tadpoles, the suprarostrals bear two small processes near its articulations with Meckel's Cartilage,

but these were not observed in Stage-41 tadpoles.

The largest and most prominent elements of the larval hyobranchium are the ceratohyalia (Figure 3). Each ceratohyal bears two anterior processes (articular or anterior process medially, and the anterolateral process laterally), one posterolateral process (processus lateralis) composing the lateral plate of the ceratohyal, and one prominent, posterior process that articulates with the hypobranchial plate. The anterolateral process is thinner and more delicate than the adjacent anterior process. A broad pars reunions unites the ceratohyalia, forming a bridge between them. Copula I is a small cartilage located anterior to the pars reunions. The pars

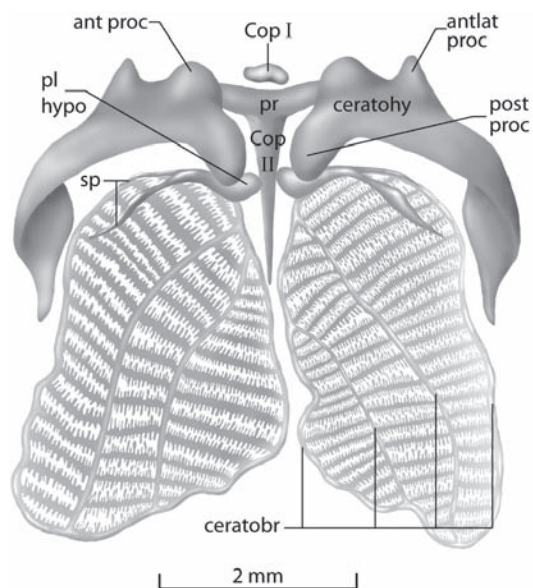


**Figure 3.** Hyobranchium of Stage-41 larva of *Gastrophyryne carolinensis* in dorsal view. Abbreviations: ant proc = anterior process; antlat proc = anterolateral process; ceratobr = ceratobranchialia; ceratohy = ceratohyal; Cop I = Copula I (basihyal); Cop II = Copula II (basibranchial); pl hypo = planum hypobranchiale; post proc = posterior process; pr = pars reunions; sp = spiculum.

reuniens seems to be continuous with medial Copula II, which separates the hypobranchial plates. The crista hyoidea or urobranchial process of the copula tapers posteriorly, extending approximately a quarter of the length of the branchial basket. The large processus lateralis of the ceratohyalia curves posterodorsally where it forms a broad, thin plate. Two long, thin, sinuous spicules project laterally from the hypobranchial

plate. The branchial basket is comprised of four thin ceratobranchials that unite distally to form the commissurae terminalis.

#### Cranial Osteology of Adults

The skull of *Gastrophryne carolinensis* is approximately as wide as it is long (Figure 4A–C). The skull is widest at the level of the jaw

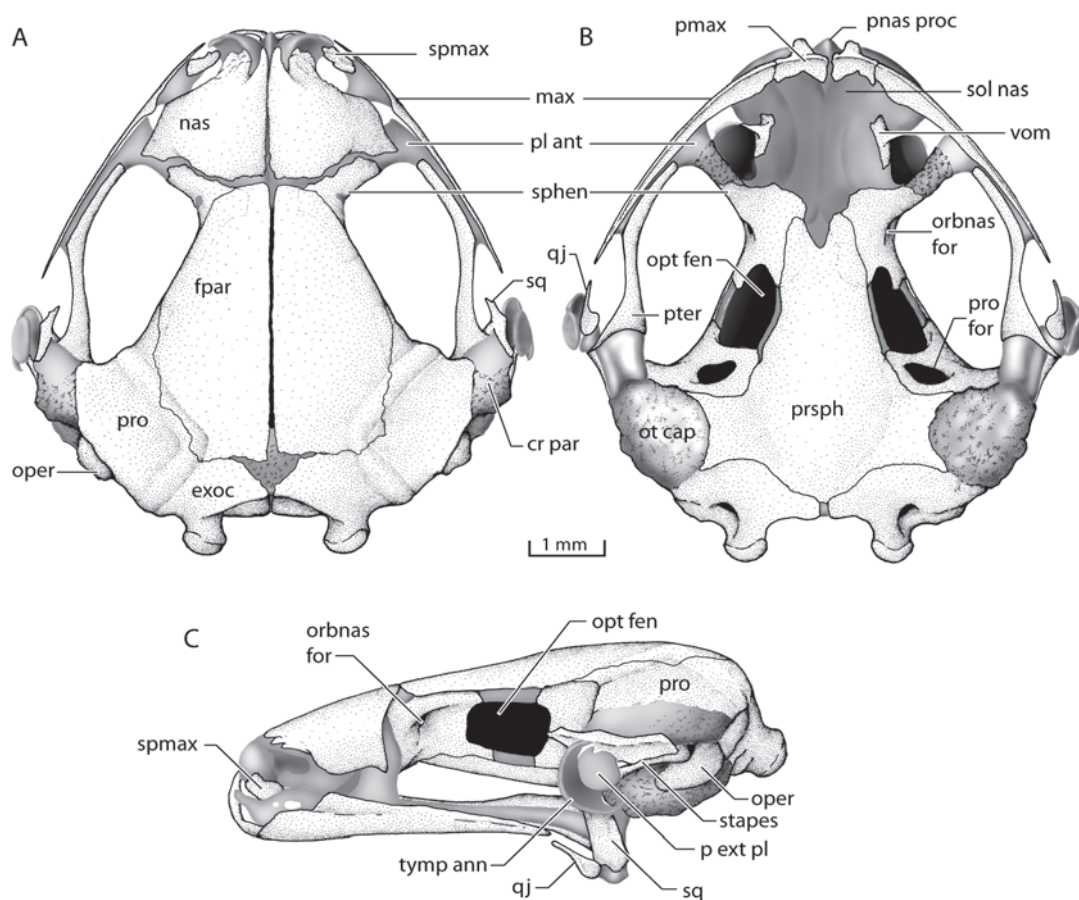


**Figure 4.** Skull of adult male *Gastrophryne carolinensis* (KU 279366) in (A) dorsal, (B) ventral, and (C) lateral views. Gray is cartilage; stippled gray is mineralized cartilage. Abbreviations: cr par = crista parotica; exoc = exoccipital; fpar = frontoparietal; max = maxilla; nas = nasal; oper = operculum; opt fen = optic fenestra; orbnas for = orbitonasal foramen; ot cap = otic capsule; p ext pl = pars externa plectri; pl ant = planum antorbitale; pmax = premaxilla; pnas proc = prenasal process; pro = prootic; pro for = prootic foramen; prsph = parasphenoid; pter = pterygoid; qj = quadratojugal; sol nas = solum nasi; sphen = sphenethmoid; spmax = septomaxillae; sq = squamosal; tymp ann = tympanic annulus; vom = vomer.

articulations, which are located extraordinarily far forward in this anuran; a transverse line projected across the skull between the ends of the upper jaw lies in the posterior part of the orbit far anterior to the otic capsule. The rostrum is large; its width is nearly 63% of the greatest width of the skull and its length is 33% of the medial length of the skull. The planum antorbitale, which forms a vertical wall separating the anterior orbit from the posterolateral part of the nasal capsule, usually is oriented approximately transversely in the dorsal/ventral aspects of the skull; however, in *G. carolinensis*, it is directed anterolaterally from the orbitonasal foramen toward the maxilla. The endocranium is incompletely ossified, but the dorsolateral and ventral regions of the otic capsule are highly mineralized. Although a moderately small frog (< 30 mm SVL), the dermal roofing bones are well developed.

*Neurocranium.*—The anterior neurocranium is composed of massive olfactory capsules, which are predominately cartilaginous and lacking obvious mineralization. There is a prominent medial prenasal process between the alary cartilages. The septomaxillae (Figure 4A, B) are unusually large bones exposed in dorsal and lateral views ventrolateral to the nasal bones. The solum nasi is completely cartilaginous and lacks mineralization. The posterolateral wall of each nasal capsule is composed of the bony sphenethmoid medially and of heavily mineralized cartilage of the planum antorbitale laterally, whereas the medial wall of the capsule is cartilaginous. There is no well-defined precebral tectum or clear separation between the olfactory capsules. In whole-mount specimens, neither superior nor inferior prenasal cartilages are visible; however, this does not preclude their presence and concealment by the premaxillae.

The paired sphenethmoids are broadly separated from one another dorso- and ventromedially. The bones form the anterolateral walls of the braincase and the anterior margins of the optic fenestra and contain the orbitonasal foramina, the margins of which are formed

completely in bone. In dorsal view, the ossification of the sphenethmoid can be seen to extend about half way toward the maxilla in the planum antorbitale.

The prootic is synchondrotically united to the sphenethmoid by cartilage in the floor and roof of the braincase; this cartilage is exposed along the lateral margins of the parasphenoid in the region of the optic fenestra (Figure 4B, C). The prootics form the posterolateral walls of the braincase, and the anterior and medial parts of the otic capsule. The posterior end of the braincase and posterior parts of the otic capsules are formed by the exoccipitals. The anterior, dorsal, and posterior walls of the otic capsule are well ossified and formed by a synostosis of the prootic and exoccipital; however, the floor of the otic capsule is heavily mineralized cartilage derived from the prootic (Figure 4B). Likewise, the crista parotica is cartilaginous, but is heavily mineralized in its posterior half. The exoccipitals are separated by cartilage ventromedially and dorsomedially by the planum basale and tectum synoticum, respectively; the tectum synoticum is heavily mineralized (Figure 4A).

The pars media plectri has a long, robust shaft that projects anterolaterally at an unusually acute angle to accommodate the anterior position of the tympanum relative to the fenestra ovalis. The footplate, or pars interna plectri, also is ossified and is slightly expanded proximally near its abutment with the operculum within the fenestra ovalis. The cartilaginous distal pars externa plectri is oval and about half the diameter of the tympanic annulus. The annulus is funnel shaped with a circular margin that is interrupted posterodorsally. The operculum is large (Figure 4C) and fills most of the fenestra ovalis; it is highly mineralized posteroventrally near its contact with the plectral apparatus.

*Dorsal investing bones.*—The large nasals extend from the level of the alary cartilages and anterior ends of the septomaxillae anteriorly, and nearly reach the frontoparietals and sphenethmoid posteriorly (Figure 4A). The bones are narrowly separated from one another medially, and extend

ventrolaterally to cover the dorsolateral regions of the olfactory capsules. The ventrolateral aspect of the olfactory capsule is exposed owing to the minimal development of the maxilla, which is broadly separated from the nasal. Dorsomedially, each nasal bears a prominent rostral process, which is flanked laterally by irregular ossification along the anterior margin that appears to be of disorganized membranous origin. The nasals lack a distinct descending maxillary process.

The expansive frontoparietals are only narrowly separated at the midline and, thus, nearly completely cover the frontoparietal fontanelle. The posterolateral corner of each frontoparietal overlaps the fused prootic and exoccipital in the medial region of the epiotic eminence. The frontoparietal is unusual in lacking any evidence of a lamina perpendicularis (Figure 4C).

*Ventral investing bones.*—The parasphenoid is robust, extending from the level of the orbitonasal foramina to slightly anterior to the foramen magnum (Figure 4B). The cultriform process is wide, with irregular margins; the base of the process is about twice the wide as the anterior end. The anterior margin of the wide cultriform process bears a V-shaped incision. The anterior and posterior margins of the short parasphenoid alae are shallowly concave, anteriorly and posteriorly, respectively. The lateral margins are also concave, seemingly accommodating the spherical ventral protrusion of the ventrolateral otic capsule.

Neopalatines are absent; the mineralization of the plana antorbitale should not be confused with the presence of a neopalatine. The vestigial vomer consists of a small basal component and a ventrolaterally directed spine, the prechoanal process that supports the anterior margin of the choana.

*Maxillary arcade.*—The edentate maxillary arcade is composed of premaxillae, maxillae, and quadratojugals. The quadratojugals are well developed, but widely separated from the posterior ends of the maxillae; thus, the upper jaw is incomplete. The maxilla and premaxilla

have modestly developed partes palatinae. The articulation of the maxilla with the premaxilla is a simple abutment with no overlap of the pars facialis of the maxilla on the premaxilla. The pars palatina of the premaxilla bears a relatively shallow incision producing a short, broad palatine process medially and a poorly defined lateral process adjacent to the maxilla laterally. There is a narrow, but obvious separation between the premaxillae medially. The alary process or pars dorsalis of the premaxilla has a slight anterior inclination and, in frontal aspect, its long axis is oriented slightly laterally. The maxilla is poorly developed, bearing a low pars facialis and lacking any indication of a preorbital process. The quadratojugals, although not large, are well ossified and lie laterally adjacent to the ventrolateral margin of the palatoquadrate cartilage. There is no mineralization of this cartilage or indication of synostosis of the quadratojugal with the dorsally adjacent squamosal.

*Suspensory apparatus.*—The pterygoid is unusual in *Gastrophryne carolinensis* and deviates from the typical triradiate configuration observed in most anurans (Figure 4A, B). The anterior ramus is robust and extends forward from the articular region in what could be described as a track that is more or less parallel to the midline of the skull, but one in which the bone shape executes a slight sigmoid twist. The anterior ramus invests the posterior maxillary cartilage along the lingual margin of the maxilla from the level of the planum antorbitale posterior through the orbit. The posterior end of the pterygoid is expanded to form a triangular plate that is oriented in a dorsoventral plane and that invests the medial surface of the palatoquadrate cartilage (Figure 4A, B). Viewed from a ventral aspect, it is apparent that the posteromedial edge of the pterygoid is blunt and lacks any remnant of a medial ramus. Typically, the medial ramus of the pterygoid extends to the anteroventral margin of otic capsule and invests the orbital margin of the basal process of the palatoquadrate (Duellman and Trueb 1994). In *G. carolinensis*, however, the margin of the posteromedial edge

of the pterygoid is displaced far forward of the otic capsule and ventromedially invests a large block of cartilage that we interpret as an enormously enlarged basal process of the palatoquadrate that supports the anteriorly displaced jaw against the anterolateral corner of the ventral part of the otic capsule.

The triradiate squamosal (Figure 4C) supports the tympanum and invests the lateral surface of the palatoquadrate. The ventral margin of the ventral ramus lies dorsally adjacent to the quadratojugal, but is not synostotically united to it. The otic ramus is about twice the length of the zygomatic ramus and articulates with the anterolateral margin of the crista parotica (Figure 1A). The short zygomatic ramus tapers anteriorly and is inclined dorsally.

**Mandible.**—The mandibles are edentate and the mandibular symphysis lacks a syndesmotic connection; the medial epiphyses of the mentomeckelian bones are united in continuous cartilage (Figure 5). The dentary invests approximately half of the anterolateral surface of Meckel's cartilage, whereas the angulosplenic invests nearly the entire medial and ventral surfaces. Whereas the dentary and angulosplenic do not articulate with one another, the mentomeckelian bone is fused to the anterior tip of the dentary. A clavate cartilage, the mentomeckelian diverticulum of de Villiers (1930), extends from the mentomeckelian bone along the lingual surface of the anterior margin of the angulosplenic bone; in some individuals, it is mineralized.

**Hyobranchial skeleton.**—The corpus of the hyoid is wider (at its waist between the anterolateral and posterolateral processes) than it is long (Figure 5) and bears three areas of mineralization—one anteromedial, and a pair located posteromedially. There is a narrow, transverse slit between the posterior margin of the hyoid corpus and the anterior margins of the bony posteromedial processes and the mineralized cartilage that lies between them; however, the corpus is united with the posteromedial processes at their anterolateral margins. The posteromedial processes are long, and relatively slender and

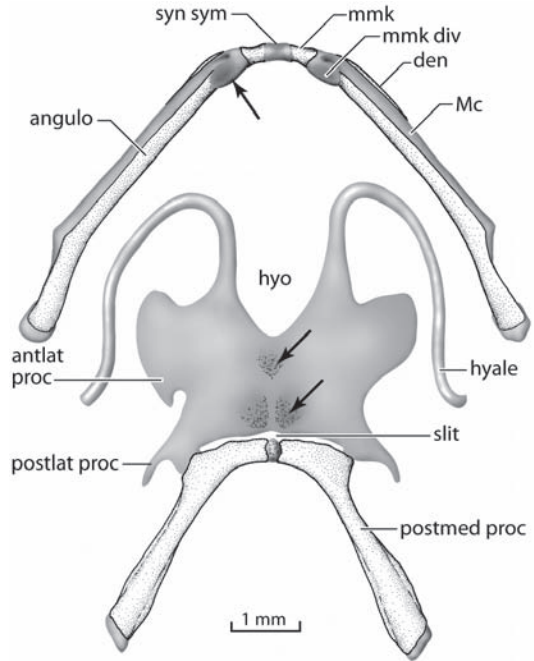


**Figure 5.** Mandible and hyoid of adult male *Gastrophryne carolinensis* (KU 279366) in ventral aspect. Arrows indicate areas of mineralization. Gray is cartilage; stippled gray is mineralized cartilage. Abbreviations: angulo = angulosplenic; antlat proc = anterolateral process; den = dentary; hyo = hyoglossal foramen; Mc = Meckel's cartilage; mmk = mentomeckelian bone; mmk div = mentomeckelian diverticulum; postlat proc = posterolateral process; postmed proc = posteromedial process; syn sym = syndesmotic symphysis.

straight, with only moderate expansion of the processes distally and development of narrow lateral flanges. Proximally, the medial portions of the heads of the posteromedial processes are greatly expanded; the bones are separated by a narrow, mineralized protuberance of cartilage. The posterolateral processes are short, slender, posteriorly curved processes. The anterolateral processes are irregular, clavate projections. The hyoglossal sinus is relatively deep and narrow; there is no evidence of a hyoglossal membrane. The hyalae are simple.

*Axial Skeleton*

The postcranial axial skeleton comprises eight presacral vertebrae, the sacrum, and the urostyle (Figure 6A). Presacrals I–VII are procoelous, whereas Presacral VIII is amphicoelous. Presacrals I and II are imbricate, and the others are non-imbricate. The vertebral profile in decreasing order of width of the bony parts is: III > sacrum > II = IV > V > VI > VII = VIII ≈ I. The transverse processes of Presacrals III and V are oriented nearly perpendicular to the midline of the body, whereas those of Presacral IV are oriented posteriorly and those of Presacrals

II and VI–VIII are directed anteriorly. The sacral diapophyses are moderately and symmetrically expanded, with the width of the base being about one third the width of the lateral margin of the bone. Densely mineralized cartilages are associated with the lateral margins of the sacral diapophyses; these cartilages extend posteriorly, and at their greatest length they range from 175–200% of the maximum distal dilation of the sacral diapophysis. The urostyle is simple, having a low dorsal crest and bearing a bicondylar articulation with the sacrum. It is approximately 90% of the length of the combined length of the sacrum and presacral vertebrae.

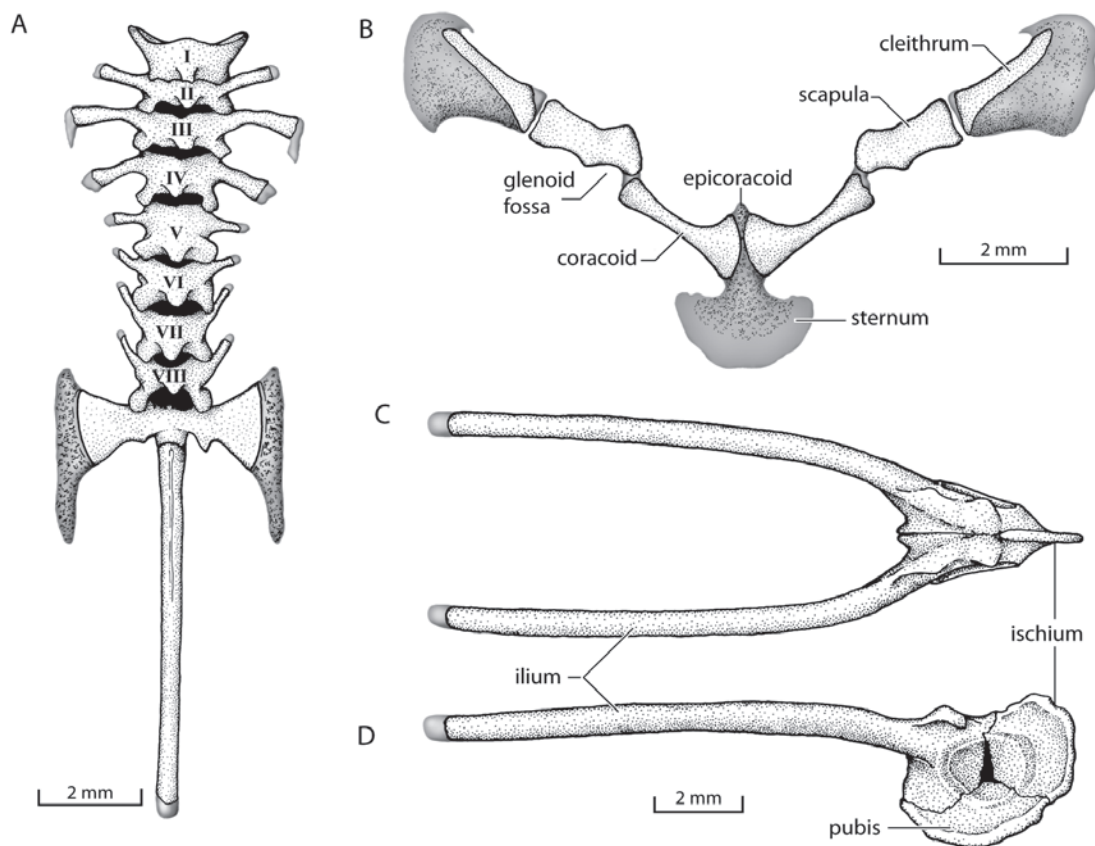


**Figure 6.** Postcranial elements of skeleton of adult male *Gastrophryne carolinensis* (KU 279366). (A) Axial column in dorsal view with presacral vertebrae numbered. (B) Pectoral girdle in ventral view with all parts deflected into the ventral plane. Dorsal (C) and lateral (D) views of pelvic girdle. Gray is cartilage; stippled gray is mineralized cartilage.

## Appendicular Skeleton

*Pectoral girdle.*—The small, firmisternal pectoral girdle has fused, indistinct epicoracoid cartilages (Figure 6B). The cartilaginous sternum is wide and flat, and synchondrotically united with the epicoracoids. Clavicles, procoracoids, and an omosternum are absent. The coracoids are long and narrowly separated medially by the epicoracoid cartilages. The width of the glenoid end of the coracoid is approximately twice that of the midshaft of the bone; the sternal end of the bone is about twice as large as the glenoid end. The coracoid is united to the scapula at the glenoid fossa by means of mineralized cartilage.

The scapula is robust, but shorter than the coracoid. The pars acromialis is well developed, but not distinctly separated from the poorly developed pars glenoidalis. The midwidth of the scapula is contained about two and one-half times within its length.

The well-ossified cleithrum, a dermal bone, lies at the anterior margin of the suprascapular cartilage, which is highly mineralized. Near its base, the cleithrum is wide and nearly extends the full length of the medial margin of the suprascapular cartilage. The cleithrum extends along approximately 95% of the anterior margin of the suprascapular cartilage and terminates in a small, rounded tip. The dorsal suprascapular cartilage expands widely such that at its maximum anteroposterior width it is approximately two and one-half times that of its medial margin. The anterior margin of the suprascapular cartilage possesses a medially directed “hook.”

*Pelvic girdle.*—The articulations between the ilium, ischium, and pubis are well defined, and all three bones participate in forming the acetabulum (Figure 6C, D). The ilium and ischium form most of the antero- and posterodorsal parts of the acetabulum, whereas the pubis forms the ventral portion. The preacetabular angle of the ilium is slightly less than 90°. The shafts of the ilia are round and smooth. In dorsal aspect, the ilia configure a narrow U-shape, with the distance between the

tips of the ilial shafts being little more than a quarter (28%) of the entire length of the element. The ilia are not fused medially. The ischia are fused medially and bear a crest along the perimeter. The pubis is thin, but ossified in this individual.

*Manus.*—The phalangeal formula is 0-2-2-3-3; the relative lengths of the digits are, as follow: IV > V > III > II (Figure 7A, B). The distal end of the terminal phalanges range from fully bilobate to weakly expanded. The carpus is composed of eight separate mesopodial bones. There is a large radiale, a smaller ulnare, and a minute intermedium that lies along the proximal and dorsal margin of the radiale (Figure 7A). Immediately distal to the radiale and ulnare, there are two bones—Element Y and a large distal carpal formed by the fusion of Distal Carpals 3–5. Distal Carpal 2 articulates with the base of Metacarpal II, the medial margin of the large distal carpal, and the distal margin of Element Y. Two ossified prepollical elements extend from the medial margin of Distal Carpal 2.

*Pes.*—The phalangeal formula is 1-2-3-4-3; the relative lengths of the digits are, as follow: IV > III > V > II > I (Figure 7C). The distal end of the terminal phalanges is generally bilobate. The tarsus is comprised of five mesopodial bones. Distal Tarsals 1, 2, and 3 are well-defined, separate elements. There are two small prehallical elements that articulate with the medial margin of Distal Carpal 1; the distal of these prehallical elements is triangular and approximately the same size as Distal Carpal 1.

## Ossification Sequence

*Endocranium.*—The paired sphenethmoid bones were observed only in adults; thus, they must ossify some time after the completion of metamorphosis.

Ossification of the exoccipital is first observed at Stage 41 (Table 1). In subsequent stages, the posterior braincase in the region of the jugular foramen ossifies. Two centers of prootic

ossification appear in Stage 42—an anterior center in the posterolateral wall of the braincase, and a second center located in the posterolateral margin of the otic capsule. The exoccipitals are completely ossified at Stage 45, whereas ossification of the prootics is not completed until after metamorphosis. The last areas of the prootics to ossify are the cristae parotica, otic capsules, and the epiotic eminences (as in the adult KU 22644). The plectral apparatus (partes plectri interna and media) ossifies after metamorphosis.

**Exocranium.**—The nasal bones begin to ossify in Stage 41 from a single ossification center that lies dorsal and medial to the nasal capsules just anterior to the orbit. As development proceeds, ossification progresses anteriorly first, and then ventrolaterally toward the pars facialis of the maxilla. Ossified septomaxillae are first visible at Stage 42 within the nasal capsules. The vomers were only observed in adult specimens, and thus, presumably ossify some time after the completion of metamorphosis.

Ossification of each frontoparietal occurs dorsal to the taenia tecti marginalis in Stage 34. By Stage 41, the bones are present as thin plates narrowly separated from one another medially and completely roofing the underlying frontoparietal fontanelle.

The parasphenoid is the first bone to ossify and is apparent at Stage 33. Two slender centers of ossification extend along the lateral margins of the neurocranial floor. By Stage 41, the parasphenoid is already well ossified, and the two elongate centers of ossification are visible ventral to the neurocranium. Ossification proceeds posteriorly with medial fusion of ossification centers and the ossification of the parasphenoid alae.

Fibrous condensations that give rise to the premaxillae are discernable at Stage 41, but ossification is not visible until Stage 42. Ossification begins along the center of each alary process and the pars dentalis ossifies later at Stage 43. The partes facialis and dentalis of the maxillae begin to ossify at Stage 44, and

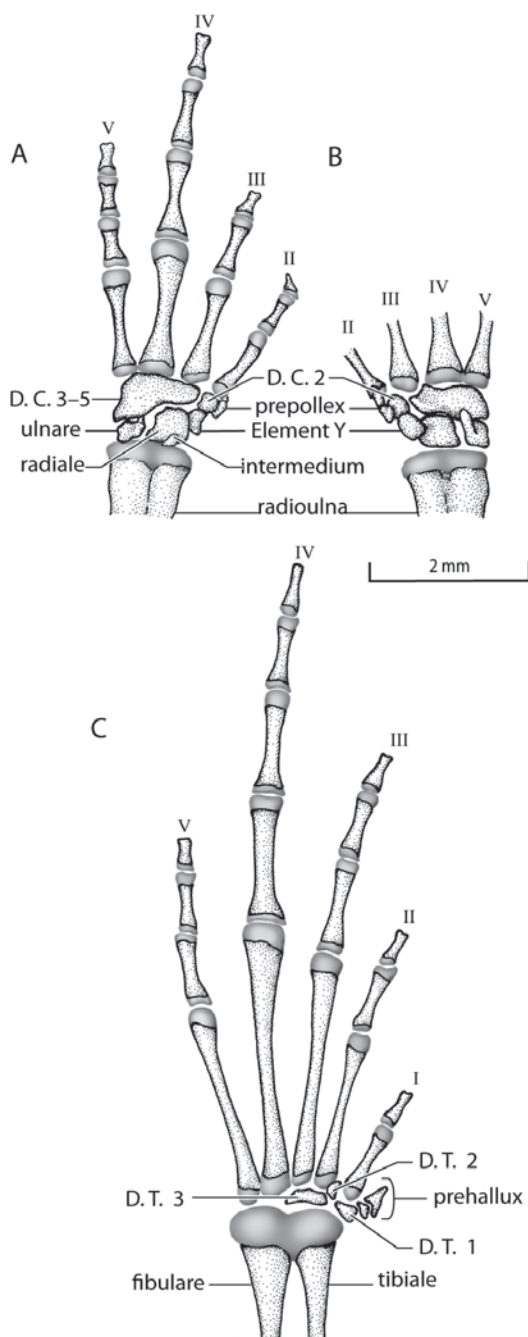


**Figure 7.** Manus and pes of adult male *Gastrophryne carolinensis* (KU 279366). (A) Dorsum and (B) venter of manus. (C) Dorsum of pes. Gray is cartilage. Abbreviations: D.C. = distal carpal; D.T. = distal tarsal.

**Table 1.** Sequence of ossification events in *Gastrophryne carolinensis*. Bold-face indicates endochondral elements, and x2 means two centers of ossification. Elements were scored at the first visibility of organized bone as revealed by Alizarin Red stain. 46+ denotes postmetamorphic development.

Stage	Cranial	Postcranial
33	Parasphenoid	<b><i>Axial column:</i></b> <b>Centra</b> <b>Neural arches</b>
34	Frontoparietal	—
37–40	—	—
41	Nasals <b>Exoccipital</b>	<b><i>Axial column:</i></b> <b>Neural arches fuse to centra</b> <b>Transverse processes on Presacrals II and III</b> <b><i>Forelimb:</i></b> <b>Humerus</b> <b>Radioulna</b> <b><i>Hind limb:</i></b> <b>Femur</b> <b>Tibiofibula</b> <b>Tibiale</b> <b>Fibulare</b> <b><i>Pectoral girdle:</i></b> <b>Scapula</b> <b><i>Pelvic girdle:</i></b> <b>Iliac shafts</b>
42	Septomaxillae Premaxillae <b>Prootic (x2)</b>	<b><i>Axial column:</i></b> <b>Neural arches of Presacral VII</b> <b>Transverse processes on Presacral IV</b> <b>Hypochord</b> <b>1<sup>st</sup> postsacral vertebra</b> <b><i>Forelimb:</i></b> <b>Proximal metacarpals</b> <b><i>Hind limb:</i></b> <b>Proximal metatarsals</b>

Table 1. Continued.

Stage	Cranial	Postcranial
43	—	<p><b>Axial column:</b></p> <p>2<sup>nd</sup> postsacral vertebra</p> <p>Neural arches complete</p> <p>Transverse process Presacral IV</p> <p><b>Hind limb:</b></p> <p>Proximal phalanges of pes</p> <p><b>Pectoral girdle:</b></p> <p>Cleithra</p> <p>Coracoids</p>
44	Maxillae	<p><b>Forelimb:</b></p> <p>Proximal phalanges of manus</p>
45	Dentary Angulosplenic Squamosal <b>Hyoid</b> (posteromedial part)	<p><b>Axial column:</b></p> <p>Fusion of postsacral vertebrae</p>
46	<b>Mentomeckelian</b> Pterygoid Quadratojugal	<p><b>Axial column:</b></p> <p>Transverse processes Presacrals V and VI</p> <p>Postsacral vertebrae fuse with hypochord</p> <p>Sacral diapophyses</p> <p><b>Fore- and hind limb:</b></p> <p>All phalangeal bones ossified.</p>
46 <sup>+</sup>	<b>Sphenethmoid</b> <b>Plectra</b> <b>Operculum</b> Vomers	<p><b>Pelvic girdle:</b></p> <p><b>Iliac portion of acetabulum</b></p> <p>Pubis mineralization</p> <p><b>Fore- and hind limb:</b></p> <p>Carpus</p> <p>Tarsus</p>

ossification continues posteriorly through metamorphosis. At Stage 45, the pars palatina is the last component of the maxilla to appear. The quadratojugal appears near the end of metamorphosis (Stage 46), immediately ventral to the squamosal and posteroventral to the maxilla.

**Mandible.**—Both the dentary and angulosplenic begin to ossify just prior to the completion of metamorphosis at Stage 45. Ossification of the mentomeckelian bone occurs slightly later at Stage 46. The direction of angulosplenic ossification spreads both anteriorly

and posteriorly, whereas that of the dentary begins posteriorly and proceeds anteriorly.

*Suspensory apparatus.*—The squamosals begin to ossify at Stage 45 in the region of the ventral ramus and continue dorsally. The otic and zygomatic rami ossify some time after the completion of metamorphosis. At Stage 46, the pterygoid begins to ossify from an ossification center that lies medially adjacent to the palatoquadrate cartilage. The anterior process invests the medial side of the pterygoid cartilage. The expansion in the area of the medial ramus appears last.

*Hyobranchial skeleton.*—The visceral body of the larval hyobranchium (branchial baskets and associated structures) are still well developed at Stage 41. By Stage 45, the adult morphology is visible but staining was incomplete in the specimens examined. At Stage 46, the hyoid apparatus is thicker and bears well-developed posterolateral processes. Ossification of the posteromedial processes begins at Stage 45, continues postmetamorphically, and culminates in the fusion of these processes at the midline.

*Axial skeleton.*—The vertebral centra and neural arches begin to ossify in Stage 33, and by Stage 41, the vertebral centra are completely ossified. The neural arches of Presacral Vertebrae I–VIII are ossified from bilateral centers of ossification and fuse dorsally. At Stage 41, ossification is present only between the two neural arches along the dorsal portion of the sacral centrum. At this stage, there is still no articulation between developing pre- and postzygapophyses. Two pairs of postsacral neural spines are present as cartilaginous elements dorsal to, but separate from, the developing hypochord. Transverse processes are present on Presacral Vertebrae I–IV.

By Stage 42, the neural spines of Presacral Vertebra VIII meet dorsally and have begun ossification. The transverse processes of Presacral Vertebra III have begun to ossify in a medial-to-lateral direction. The pre- and postzygapophyses of the presacral vertebrae continue to grow toward one another, but remain separate. The

centrum of the sacral vertebrae is not completely ossified ventrally. Ossification is also visible in the lateral portion of the two pairs of postsacral neural spines, the cartilages of both of which meet dorsally. At this stage, ossification is also first observed in the hypochord.

By Stage 43, the dorsal parts of the neural arches are ossified, but the arches are not united with their respective centra. The transverse processes of Presacral Vertebra IV are ossified. At this stage, the sacral diapophyses are first visible as cartilaginous rods projecting laterally from the sacral neural arches. The postsacral neural spines and hypochord are all present as well-defined, separate ossifications.

At Stage 44, both the transverse processes of Presacral Vertebra V and the sacral diapophyses have elongated; the latter are located anterodorsally to the elongating shafts of the ilia. The presacral and sacral zygapophyses articulate with one another. The ventral portion of the centrum of the sacral vertebrae remains unossified, but now abuts the anterior surface of the developing urostyle.

By Stage 45, the dorsomedial portion of the neural arch of the atlas is broad and tapers posteriorly. In general, the shape of the dorsal portions of the neural arches has changed such that they are expanded both anteriorly and posteriorly, and flattened dorsoventrally. The sacral centrum still is not fully ossified. The sacral diapophyses reach the ilial shafts laterally, but are not ossified. The postsacral neural spines bear posterolateral projections that extend toward the hypochord. Tail resorption is complete at this stage and further ossification and morphogenesis in the urostyle must occur after metamorphosis.

After the completion of metamorphosis at Stage 46, ossification is present at the most proximal part of the sacral diapophyses. The postsacral neural arches are nearly in contact with the dorsally expanding hypochord. Transverse processes are first visible on Presacral Vertebra VI.

*Appendicular skeleton.*—By Stage 41, the cartilaginous components of the pectoral girdle

(coracoids, scapulae, and suprascapulae) are well developed and the epicoracoid cartilages are fused. Ossification of the pectoral girdle begins at Stage 41 with a single ossification center in each the scapula; ossification is evident in the coracoid and the cleithrum at Stage 43. There is no evidence of the presence of clavicles, procoracoid cartilage, or an omosternum at any stage of ontogeny. At Stage 44, the sternal cartilage is present and the most distal part of the cartilaginous suprascapula has expanded distally as well as anteriorly and posteriorly. Ossification of the coracoid and scapula is nearly complete at Stage 46. The cartilage separating the coracoid and scapula in the region of the glenoid fossa is highly mineralized in adults. The anterior epicoracoid cartilage is highly mineralized, especially near the coracoids. Further development in the suprascapular cartilages occurs after metamorphosis as the suprascapula in adults is curved medially at the anterodistal portion of the suprascapula adjacent to the distal tip of the cleithrum.

By Stage 41, the ilial shafts of the pelvic girdle are well developed and nearly reach the sacrum anteriorly. Each shaft has a single center of ossification that lies proximal to the acetabulum. Ossification of the ilial portion of the acetabulum begins at Stage 45, whereas that of the ischial portion begins after metamorphosis at Stage 46. The left and right halves of the pelvic girdle remain relatively well separated medially throughout larval development. Mineralization of the pubis begins at Stage 46 but, along with the remaining pelvic girdle, continues after metamorphosis.

The long bones of the limbs are already well ossified at Stage 41. The metacarpals and metatarsals are the last limb elements to begin ossification at Stage 42. Between Stages 43 and 46, the phalanges ossify, with those of the foot preceding those of the hand. The carpal and tarsal elements remain cartilaginous throughout larval development and only are ossified in larger, presumably older, adults. The prepollical and prehallical elements are highly mineralized.

## Discussion

Owing to the lack of parity in taxon sampling and genetic loci in the two published analyses of microhylid relationships (Frost *et al.* 2006, van der Meijden *et al.* 2007), we conducted a phylogenetic analysis combining data from these and other recent studies (e.g., Von Bocxlaer *et al.* 2006, Roelants *et al.* 2007, Wollenberg *et al.* 2008) to generate a phylogenetic framework for discussing morphological diversity. As shown in Figure 8, the monophyly of Microhylidae is strongly supported, as it is in earlier studies. In our estimate of phylogeny, the Asian genus *Kalophryne* and the African genus *Phrynomantis* may be the earliest branching lineages within the Microhylidae. Because of the low support values, all major lineages of microhylids essentially form a polytomy among the recognized subfamilies. Of the subfamilies represented by more than one taxon, the African Phrynomerinae, the Malagasy Scaphiophryinae, Cophylinae, and Dyscophinae, the Gastrophryninae of the New World, and the Australasian Asterophryninae, all have robust support. While the Microhyliinae is resolved as monophyletic, this does not receive strong support. As in other recent studies, the south Asian genus *Kaloula* is not resolved as monophyletic (Van Bocxlaer *et al.* 2006, D. C. Blackburn, C. D. Siler, J. A. McGuire, D. C. Cannatella, and R. M. Brown unpubl. data). Several sister relationships resolved in our analysis that do not receive strong support still seem to make sense biogeographically—e.g., the sister relationship between the African Hoplophryninae and the Malagasy Scaphiophryninae and Cophylinae, and the sister relationship between two enigmatic South American genera, *Otophryne* and *Synapturanus* (though *RAG-1* is the only locus sampled for both taxa). We resolved nearly all relationships within the monophyletic Gastrophryninae with robust support, which facilitates our morphological comparisons below.

In our analysis as in Frost *et al.* (2006) and van der Meijden *et al.* (2007), the New World gastrophrynines are monophyletic. However, the relationships of all 18 genera cannot be depicted



owing to lack of molecular data for five genera (*Stereocylops*, *Hyophryne*, *Arcovomer*, *Adelastes*, and *Relictivomer*) and lack of taxon parity in analyses. To provide a more complete scheme of relationships for discussion, we have integrated the results of Greenbaum's (2006) analysis with ours (Figure 9); these were not included in our analysis because the data are unpublished and unavailable in GenBank.

### Features of Larval Morphology

The chondrocrania of only 10 microhylids have been described in detail, in addition to the present work. De Sá and Trueb (1991) compared features of *Hamptophryne boliviana* with the two other New World microhylids—*Otophryne robusta* (Wassersug and Pyburn 1987) and *Elachistocleis bicolor* (Lavilla and Langone 1995, Vera Candioti 2007). The chondrocranium of *Dermatonotus muelleri* was described by Lavilla (1992) and Vera Candioti (2007), and those of *Chiasmocleis panamensis* and *C. leucostica* by Vera Candioti (2006, 2007) and Langone *et al.* (2007), respectively. In addition, the chondrocrania of three Old World microhylid taxa are known—*Uperodon systoma* and *Microhyla ornata* (Ramaswami 1940), and *Kaloula pulchra* (Haas 2003).

In his paper describing the mandibular arch musculature of anuran larvae, Haas (2001) described an apomorphic feature of the jaw musculature of the microhylid larvae that he examined—the m. levator mandibulae longus profundus does not overlap the m. l. m. l. superficialis posteriorly. He also noted that the m. levator mandibulae longus profundus has an anterior origin near the m. levator mandibulae externus. The anterior origin of this muscle distinguishes *Elachistocleis*, *Gastrophryne*, and *Kaloula* from *Scaphiophryne madagascariensis*, in which the m. l. m. longus has a posterior origin. Haas (2003) cited 14 additional larval morphological characters of *Scaphiophryne* that he considered plesiomorphic, and described five larval traits (most of which are related to suspension feeding) distinguishing New World

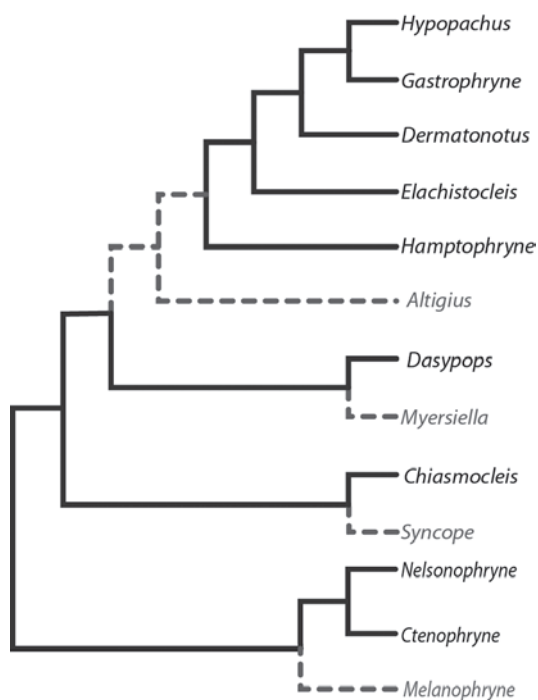


**Figure 9.** Simplified phylogeny of Gastrophryninae including placement (broken gray lines) of taxa studied by Greenbaum (2006).

microhylids (*Gastrophryne*, *Hamptophryne*, and *Elachistocleis*) from Old World taxa.

Chondrocranial features of some of the taxa of microhylids that have been examined are summarized in Table 2. *Otophryne* lacks an ascending process, and possesses a taenia tecti medialis, long cornua trabeculae, and inverted muscular process of the palatoquadrate; this suite of characters distinguishes it from larvae of both Gastrophryninae and Microhyliinae and supports the results of molecular phylogenetic analyses that do not resolve *Otophryne* as members of these clades. Further, there are some interesting commonalities shared by the other nine taxa (*Dermatonotus muelleri*, *Chiasmocleis panamensis*, *C. leucosticta*, *Elachistocleis bicolor*, *Hamptophryne boliviana*, *Gastrophryne carolinensis*, *Kaloula pulchra*, *Microhyla ornata*, and

**Table 2.** Comparison of chondrocranial features of microhylid frogs. Data for *Gastrophryne carolinensis* (this study), *Chiasmocleis panamensis* (Vera Candiotti 2006), *C. leucosticta* (Langone et al. 2007), *Elachistocleis bicolor* (Lavilla and Langone 1995), *Hamptophryne boliviana* (de Sá and Trueb (1991), *Otophryne robusta* (Wassersug and Pyburn 1987), *Kaloula pulchra* (Haas 2003), and *Microhyla ornata* and *Uperodon systoma* (Ramaswami 1940).

Chondrocranial character	Gastrophryninae					?		Microhylinae	
	<i>Gastrophryne</i>	<i>Chiasmocleis</i>	<i>Dermatonotus</i>	<i>Elachistocleis</i>	<i>Hamptophryne</i>	<i>Otophryne</i>	<i>Kaloula</i>	<i>Microhyla</i>	<i>Uperodon</i>
Taenia tecti medialis	-	-	-	-	-	+	+	-	-
Superior labial cartilage(s) fused with cornu trabeculae	+	+/-	+	+	-	-	-	-	-
Superior labial cartilage single	+	+	+	+	-	+	+	+	+
Cornu trabeculae	Short	Short	Short	Short	Short	Long	Short	Short	Short
Inferior labial cartilage	Single	Single	Single	Single	Paired	Single	Paired	Single	Single
Muscular process	Low, dorsal	Low, dorsal	Low, dorsal	Low, dorsal	Low, dorsal	Low, ventral	Low, dorsal	Low, dorsal	Low, dorsal
Subocular fenestra	Length 2x width	Length 2x width	Length 2x width	Length 2x width	Length 4x width	Length 3x width	Length 2x width	Length 1.25x width	Length 2x width
Ascending process	+	+	+	+	+	-	+	+, broad	+
Subpalatoquadrate bar	-	-	-	-	+	-	-	-	-
Posterolateral process	+, elaborated posteriorly	+, elaborated posteriorly	+	+	+, part of subpalatoquadrate bar	+	+, expanded anteriorly	+	+
Subotic quadrate process	+	+	+	+	+	-	+	-	-
Crista parotica	+, fenestrate	-	+, fenestrate	-	+, fenestrate	+, fenestrate	+	-	-

*Uperodon systoma*). In dorsal and ventral profiles, the chondrocrania of these taxa are notably wide at the posterior level of the palatoquadrate, anterior to the otic capsules; this doubtless is correlated with the elaboration of a posterolateral process of the palatoquadrate. In most other anuran larvae, which lack a posterolateral process, the chondrocranium at the posterior level of the palatoquadrate is about equal in width, or only slightly wider, than the width at the level of the muscular process, and the greatest width may be at the mid-orbital level (e.g., *Lithobates sylvaticus* [Larson 2002; *Rana sylvatica* auctorum] or *Anaxyrus americanus* [Larson 2004; *Bufo americanus* auctorum]). The frontoparietal fontanelle (and cranial cavity) in gastrophrynine and microhylid taxa tends to be short and wide, and the muscular process of the palatoquadrate poorly developed. All have short cornua trabeculae diverging from a relatively long ethmoid plate. The superior labial cartilage or suprarostrals is a single element in all except *Hamptophryne*. In all, the infrarostrals or inferior labial cartilage(s) form a keyhole-shaped structure, and in most, the cartilage is single, rather than paired (contra the interpretation for *Hamptophryne* of de Sá and Trueb 1991). Haas (2003) cited four chondrocranial/hyobranchial characters that are shared by gastrophrynines and that distinguish them from other microhylids—*Kaloula pulchra* (Microhylinae) and *Phrynomantis bifasciatus* (Phrynomerinae). These are: (1) the division of origin of the m. levator arcuum branchialium III into two bundles that cross one another before converging into the flat distal part of the muscle; (2) the connection of the dorsal margin of the muscular process to the neurocranium by only a ligament; (3) the presence of a conspicuous ventrolateral projection from the anterolateral base of the muscular process; and (4) the absence of a ligament joining Meckel's cartilage to the superior labial cartilage. The third feature is present in *Elachistocleis bicolor* (Vera Candioti 2007), but we did not observe the third feature in *Gastrophryne* (or in other New World taxa that have been illustrated

except *E. bicolor*). Nonetheless, there remain three chondrocranial characters in support of the monophyly of the New World gastrophrynine microhylids represented by *Elachistocleis*, *Gastrophryne*, and *Hamptophryne* morphology (Haas 2001, 2003).

#### *Osteological Features of the Adults*

*The dimensions of the challenge.*—New World microhylids are a disparate assemblage of numerous genera, most of which contain few species and many of which are characterized by peculiarities of the adult skeletal morphology. As presently understood (Frost 2011), Gastrophryninae comprises at least 13 genera (number of species in parentheses)—*Altigius* (1), *Chiasmocleis* (25), *Ctenophryne* (2), *Dasytops* (1), *Dermatonotus* (1), *Elachistocleis* (6), *Gastrophryne* (5), *Hamptophryne* (1), *Hypopachus* (2), *Melanophryne* (2), *Myersiella* (1), *Nelsonophryne* (2), and *Syncope* (3). Too little is known about the remaining New World microhylid genera—*Hyophryne* (1), *Stereocyclops* (2), *Synapturanus* (3), *Adelastes* (1), *Arcovomer* (1), and *Relictivomer*—to place them in a subfamily. There is partial osteological information for 23 taxa of the 61 species of New World microhylids. The most complete accounts are those for *Hamptophryne boliviana* (de Sá and Trueb 1991), *Melanophryne carpish* and *M. barbatula*, and *Nelsonophryne aterrima* and *N. aequatorialis* (Lehr and Trueb 2007), and *Gastrophryne carolinensis* (this study). The other accounts are, at best, anecdotal and incomplete. Carvalho (1948) figured ventral views of the crania, the pectoral girdles, and vertebral columns of *Stereocyclops incrassatus* and *Dermatonotus muelleri* [*Hypopachus mülleri* auctorum]; in a subsequent paper, Carvalho (1954) provided brief osteological notes and figures of the palatal region of the skull and pectoral girdles for some of the following taxa: *Hyophryne histrio*, *Hamptophryne boliviana*, *Arcovomer passerellii*, *Nelsonophryne aterrima* [*Glossostoma aterrimum* auctorum], *Dermatonotus muelleri*, *Relictivomer pearsei*, *Elachistocleis*

*ovalis* and *E. bicolor*, *Dasylops schirchi*, *Myersiella subnigra*, and *Synapturanus mirandaribeiroi* [*S. microps* auctorum]. In his description of *Adelastes hylonomos*, Zweifel (1986) illustrated the skull and hyoid, and part of the vertebral column and pectoral girdle of this taxon and compared some of its osteological features with other South American microhylids (*Hamptophryne*, *Chiasmocleis*, *Elachistocleis*, *Nelsonophryne* [*Glossostoma* auctorum], *Ctenophryne*, and *Synapturanus mirandaribeiroi*). Likewise Walker (1973) and Walker and Duellman (1974) provided some osteological information in the descriptions of *Syncope antenori* and *Chiasmocleis anatipes*, respectively, and da Silva and Meinhardt (1999) described osteological features of *Syncope tridactyla*. The most recent application of osteological data in a phylogenetic study of New World microhylids is that of Wild (1995), who described *Altigius alios*.

A review of this literature, accompanied by a reexamination of available specimens (Appendix I), allows us to make some generalizations about osteological similarities and variation among the New World microhylids. The reader is cautioned, however, that little is known about three genera for which no specimens were available for examination; these are *Dasylops*, *Stereocyclops*, and *Synapturanus*, which are only known from partial descriptions in the literature, as noted above. Based on our phylogeny (Figure 8) and Frost *et al.* (2006), *Synapturanus* is not a gastrophrynine, and nothing is known about the phylogenetic placement of *Stereocyclops*. The characters discussed below are derived from the literature cited above and our own observations. Appendix 1 summarizes these characters and the species in which they were observed; unless otherwise specified, observations apply to all species examined in a genus.

**Cranial features.**—In most New World taxa, the skull is broader than long (Appendix III); this is most pronounced in *Stereocyclops incrassatus*, which is the only known taxon in which the angle of the jaw lies at or near the posterior margin of the otic capsule. In *Adelastes*,

*Altigius*, *Chiasmocleis*, and *Syncope*, the width of the skull is about the same as the length, whereas in *Elachistocleis*, *Gastrophryne*, and *Myersiella*, the skull is narrower than long. The maxillary arcade is short, with the angle of the jaw lying either anterior to the otic capsule or at the anterior margin of the capsule in most (Appendix III); *Hamptophryne* and *Melanophryne* have moderately long maxillary arcades in which the angle of the jaw lies at the midlevel of the otic capsule. In microhylids with short maxillary arcades, the medial ramus of the pterygoid is reduced or absent and the basal process is elaborated into a massive block of cartilage at the anterolateral margin of the otic capsule, as we observed in *Gastrophryne carolinensis*. Although the maxillary arcade it is incomplete in many New World microhylids, a quadratojugal is present in all taxa except *Syncope*; the element is vestigial in *Elachistocleis cesarii*. All New World microhylids are edentate.

Many taxa have protuberant snouts in which the premaxillae are inclined anteriorly to varying degrees and the mouth is subterminal. The presence of a median prenasal process (an extension of the septum nasi) is correlated with the anterior position of the snout in all taxa except *Adelastes*, *Arcovomer*, and *Hypopachus*. *Melanophryne* and *Nelsonophryne* are exceptional. None has a markedly protuberant snout; however, all but *Melanophryne barbatula* has a median prenasal process. The sphenethmoid is represented by two separate ossifications in all taxa except *Adelastes* and *Synapturanus*; in both of the latter, the hyperossification/mineralization of the endocranium obscures the condition of the sphenethmoid.

The mandibles of all of New World microhylid taxa that we examined are united in cartilage anteromedially and lack a syndesmotomic symphysis; thus, the medial termini of the mentomeckelian elements are united by a common bridge of cartilage (contra de Sá and Trueb 1991), and lack a ligamentous or dense connective tissue separation between the halves of the mandible as is typical of most other basal and neobatrachian anurans. All

microhylid taxa have a so-called Meckelian diverticulum (of de Villiers, 1930), a cartilaginous spur of the posterolateral part of the mentomeckelian bone. This diverticulum or spur extends along the lingual surface of the anterior end of the angulosplenial bone; the cartilaginous spur is mineralized along its lingual margin in all taxa, with the extent of the mineralization depending on the taxon.

The most variable part of the New World microhylid cranium is the palate (Appendix III), with differences involving the presence, absence, and fusion of the neopalatine, and the condition of the vomer (single versus divided) and the relationships of the vomer with adjacent elements. The neopalatine is an independent element in only four genera—*Arcovomer*, *Hamptophryne*, *Melanophryne*, and *Nelsonophryne*; these taxa also have skulls that are broader than long. The neopalatine of *Hamptophryne* is reduced, and in *Arcovomer*, the neopalatine articulates with the fused posterior vomers and is clearly separate from the maxilla laterally. The neopalatine is present and illustrated by Carvalho (1954) as fused to the vomer in *Stereocyclops*, but it is absent in the remaining taxa (contra Walker 1973). *Melanophryne* and *Nelsonophryne* are closely related and compose an early branch in the Gastrophryninae (Figure 9), but the presence of an independent neopalatine in *Hamptophryne* suggests either multiple independent losses or a reappearance of this element. The vomer lacks a dentigerous process in all New World microhylids, and in most, is represented by a single bone that supports the anterior and anteromedial margins of the choana. In *Adelastes* and *Synapturanus mirandaribeiroi*, the vomer is single but extends posteriorly along the medial margin of the choana to terminate in the region of the sphenethmoid. Both Zweifel (1986) and Carvalho (1954) illustrated the vomers of these taxa as fused with the sphenethmoid; although we could not examine *Synapturanus*, we did examine *Adelastes*, and the posterior end of the vomer does not seem to be fused to the mineralized sphenethmoid region of the skull.

Walker (1973) described and illustrated the vomer of *Syncope antenori* as being divided with the posterior tip being fused to the sphenethmoid and separated from the anterior portion of the bone; our reexamination of the same specimen shows only an anterior vomer. In *Relictivomer pearsi* and *Hamptophryne boliviana*, the vomer is divided into widely separated anterior and posterior portions; the posterior vomer is a minute bone that lies anterior to the parasphenoid and sphenethmoid at the level of the planum antorbitale and seems independent of the sphenethmoid. *Arcovomer* differs from all other gastrophrynines, in having a divided vomer, in which the posterior elements seem to have fused medially across the floor of the braincase anterior to the parasphenoid.

*Hyoid*.—Not a great deal is known about the hyoids of New World microhylids, but some unusual features are worth noting. In all taxa, the posteromedial processes are stout, irregularly shaped bones, rather than the slender, symmetrical processes typical of most other neobatrachians. The proximal ends of the processes are robust; in many taxa, the heads of these processes are elaborated medially toward one another along the posterior margin of the hyoid corpus. The separation is moderately wide in *Melanophryne* and *Nelsonophryne*, and narrow in *Gastrophryne* and *Adelastes*; in *Hamptophryne*, the heads of the posteromedial processes are fused to one another medially. One of the most curious traits is the existence of a transverse slit that extends across the corpus of the hyoid adjacent to the anterior margins of the heads of the posteromedial processes in *Gastrophryne*, *Syncope tridactyla*, *Dermatonotus*, and *Hamptophryne* (contra de Sá and Trueb, 1991; Appendix III). The separation between the hyoid corpus and the posteromedial processes is so narrow in some taxa as to be inconspicuous, but does completely separate the anterior and posterior parts of the hyoid plate. A narrow, lateral band of cartilage forms a bridge between the posterolateral and posteromedial processes, thereby preserving the integrity of the hyoid corpus. In the microhylids examined here,

these bones are stout, tend to have a concave lateral margin, and are irregularly expanded in their posterior portions. Flanges along the medial margin of the process may be narrow and long (e.g., *Gastrophryne*) or an acuminate process (*Adelastes*); the more usual configuration seems to be broad, irregular expansions along the medial margin of the process (*Melanophryne*, *Nelsonophryne*, *Hamptophryne*, *Dermatonotus*, *Hypopachus*).

The corpus of the hyoid usually is mineralized and may bear one or more spinous or spur-like ventral protuberances. The hyperossified frog, *Adelastes hylonomos*, possesses a parahyoid bone (Zweifel 1986) and *Dermatonotus muelleri* has densely mineralized cartilage in the anteromedial part of the hyoid corpus. Similar, but less dense areas of mineralization, occur in *Hamptophryne*, *Melanophryne*, *Nelsonophryne*, *Gastrophryne*, and *Syncope antenori*.

The occurrence of ventral protuberances is sporadic; these may be present in the central part of the corpus and/or posteriorly, between the heads of the posteromedial processes. No protuberances are observed in *Syncope* and *Melanophryne barbatula*. There is a single, central, medial protuberance in *Adelastes* and *Nelsonophryne aterrima*, and there is a pair of protuberances (medial anterior and medial posterior between heads of posterolateral processes) in *Nelsonophryne aequatorialis* and *Melanophryne carpish*; in *Hamptophryne*, there is a posterior protuberance that is ossified with the laterally adjacent heads of the posteromedial processes.

*Axial osteology*.—Most of the New World microhylids have eight free presacral vertebrae (Appendix III). In one, *Melanophryne carpish*, Presacrals I and II are fused; thus, there are only seven free presacral vertebrae. Both species of *Syncope* have only six free presacrals. Presacrals I and II are fused in *Syncope*, and the sacrum is composed of a pair of vertebrae, indicating that a posterior presacral vertebra has been incorporated into the sacrum. Based on the pattern of phylogenetic relationships (Figure 9), this

suggests multiple origins of vertebral fusion in this Gastrophryninae. In four taxa (*Syncope*, *Synapturanus*, and *Myersiella*), there are vestigial transverse processes on the urostyle; these are well developed in all but *Myersiella*. In 10 taxa, the last presacral is amphicoelous (and the vertebral column therefore diplasiocoelous), whereas in seven other taxa, the vertebrae are procoelous (Appendix III); however, nothing is known about the intraspecific variation of this feature.

*Pectoral girdle*.—One of the most peculiar and enigmatic parts of microhylid skeletons is the pectoral girdle, the anterior parts of which are reduced or absent in most taxa. So far as is known, the clavicle is present and complete (i.e., extends from an articulation with the scapula medially to the region of the epicoracoid cartilage) in only two American taxa—*Dermatonotus muelleri* and *Stereocyclops incrassatus*. In the latter, as well as in all other known taxa, prezonal elements are absent and the midzonal portion of the girdle is abbreviated, such that the anteromedial end of the zonal portion of the girdle lies near the coracoids and far posterior to the level of the pars acromialis of the scapula. The coracoids tend to be robust, and moderately to markedly expanded medially in many taxa (e.g., *Chiasmocleis albopunctata*, *Dermatonotus*, *Nelsonophryne*). The coracoid is fused to the scapula in at least two taxa, *Hamptophryne* and *Adelastes* (Appendix III). In addition, all taxa have an expanded, plate-like sternum that usually is heavily mineralized.

Reduction of the zonal elements is manifest in several different configurations. In the most complete form, the epicoracoid cartilage is united to the procoracoid cartilage, which is complete and invested by a clavicle along its anterior margin. But the procoracoid cartilage and clavicle extend posterolaterally only to about the mid-length of the anterior margin of the coracoid, rather than anterolaterally toward the pars acromialis of the scapula. The procoracoid cartilage is complete to the mid-coracoid in *Melanophryne carpish* and *Hyophryne histrio*

(Appendix III); it is narrowly separated from the coracoid in *M. barbatula* and *Elachistocleis* sp. (Zweifel 1986). In *Chiasmocleis albopunctata*, *C. anatisipes*, and *Syncope tridactyla*, the procoracoid cartilage is complete to the mid-coracoid; note that in Figure 2 of Walker and Duellman (1974), the procoracoid cartilage is shown as not reaching the coracoid. However, because the epicoracoid cartilage is incomplete in *Chiasmocleis* and *Syncope*, the medial parts of the procoracoid and the clavicles are united only by undifferentiated connective tissue to the posterior parts of the girdle. The morphological similarity in the pectoral girdles of *Chiasmocleis* and *Syncope* support a close phylogenetic relationship between these genera (Greenbaum 2006). In three taxa (*Hamptophryne*, *Elachistocleis skotogaster*, and *Arcovomer*), the midsection of each procoracoid cartilage is absent. In this configuration, there is a lateral remnant of the cartilage associated with the lateral end of the clavicle at its terminus at the mid-coracoid, and a medial remnant associated with the medial end of the clavicle. The paired medial remnants of the procoracoids are fused to one another and the epicoracoid bridge that unites the coracoids posteriorly in *Hamptophryne*, *Elachistocleis ovalis*, *E. skotogaster*, and *Arcovomer*. *Elachistocleis ovalis* differs from its congener *E. skotogaster* in retaining only the medial portion of the procoracoid cartilage, a trait also found in *Dermatonotus muelleri*. In all the aforementioned taxa, the clavicle is short and slender, and the medial ends are broadly separated from one another. The remaining taxa lack any vestige of the procoracoid cartilage and clavicle.

**Pelvic girdle.**—The pelvic girdle is unremarkable in the few taxa for which illustrations exist (*Gastrophryne*, *Nelsonophryne*, *Melanophryne*, and *Hamptophryne*). The ilial shafts are long and slender and lack an obvious flange in all of these except *Melanophryne carpish*, which has shorter ilia that are broadly separated from one another at their distal ends; in this taxon there is low flange along the posterolateral margin of the ilial shaft. There is a well-developed, broad-based

dorsal prominence on the ilium. The acetabula are round. The preacetabular area is well developed and forms an acute angle with the ilial shaft in lateral aspect. The pubis is cartilaginous, but mineralized in all.

**Manus and pes.**—The phalangeal formula for all New World microhylids is 2-2-3-3 except in *Syncope tridactyla*, in which Digits II, III, and V are reduced and the phalangeal formula is 1-1-3-1. Distal Carpals 3–5 are fused in all except *Nelsonophryne*, in which Distal Carpal 3 is free, and Carpals 4 and 5 are fused. There is considerable variation in the shape of the terminal phalanges. They are T-shaped in *Arcovomer*, and slightly bilobate in *Altigius*, *Chiasmocleis anatisipes*, *Hamptophryne*, *Melanophryne*, *Nelsonophryne aterrima*, and *Syncope antenori*. Slightly bulbous terminal phalanges occur in *Ctenophryne geayi*, *Dermatonotus*, *Hyophryne*, *Hypopachus variolosus*, *Myersiella*, and *Stereocyclops incrassatus*. In the remaining taxa the phalanges are only slightly differentiated, and narrow and rounded.

Reduction of the toes is more common than that of the fingers. The phalangeal formula of the foot of *Syncope tridactyla* is 1-2-3-4-2; that of *Syncope antenori* is 1-2-3-4-3. The remaining taxa share the 2-2-3-4-3 formula that is typical for many anurans.

#### *Comparisons with Phrynomerinae*

In comparison to other microhylid frogs, the morphology of the microhylid subfamily Phrynomerinae (comprised of the five species of *Phrynomantis* [*Phrynomerus auctorum*] endemic to sub-Saharan Africa) has been studied extensively (de Villiers 1930, Myers *et al.* 2004). The relationship of this subfamily to New World microhylids is not clear; but in our analysis and that of Frost *et al.* (2006), Phrynomerinae seems to occupy a basal position (Figure 8), whereas van der Meijden *et al.* (2007) show it as the sister taxon of the Gastrophryninae. Despite this lack of resolution, we find comparisons between *Phrynomantis* and New World microhylids to be fruitful because of recent studies of the functional

morphology of *Phrynomantis* (Myers *et al.* 2004) and the morphological similarities of this genus to the New World taxa.

De Villiers (1930) first reported the union of the mentomandibular bones of the lower jaw in cartilage (de Villiers 1930: text-figure 12a). Devanesan (1922) first described the extension of the lateral epiphysis as a cartilaginous bar along the anterolingual margin of the lower jaw, and Emerson (1976) summarized the taxonomic distribution of this structure from the literature and illustrated the diverticula of three microhylids. De Villiers termed this structure the Meckelian diverticulum; he noted that it was mineralized along its lingual surface and served as a surface for the insertion of the m. submentalis, the m. hyoglossus, and the medial part of the m. geniohyoideus lateralis. The author commented on the modification of the submandibular musculature relative to that which he had observed in other anurans, reporting that the enlargement of the m. submentalis separates the pair of mm. hyoglossi. Further he described the m. geniohyoideus medialis as lying medial to both the m. hyoglossus and m. geniohyoideus lateralis, rather than ventral to these muscles as it does in the other anurans he had studied.

Emerson (1976) described conditions of accessory slip development and insertions of the intermandibularis posterior in several New and Old World microhylid taxa. She reported that these slips variably insert on the posterolateral edge of the submentalis, the posterolateral margin of the mentomeckelian, and the lateral margin of the diverticulum. In their study of tongue protraction in *Phrynomantis bifasciatus*, Meyers *et al.* (2004) also discussed mandibular musculature; as depicted in their drawing (Meyers *et al.* 2004:Fig. 3B), the anterior slip inserts along the mentomeckelian and Meckelian diverticulum ventral to the m. submentalis, whereas the posterior accessory slip extends to this area dorsal to the m. submentalis. Although de Villiers (1930) apparently did not notice these accessory slips, he speculated that the elaboration of the Meckelian diverticulum probably occurred in

response to a need for a strong attachment of muscles, especially the submentalis and the m. geniohyoideus lateralis. The mm. geniohyoideus medialis and lateralis originate from the mandibular symphysis and Meckelian diverticula; they extend posteriorly to insert on the posteromedial and posterolateral processes, respectively, of the hyoid. Contraction of these muscles pulls the hyoid forward raising the floor of the oral cavity; they act antagonistically with the mm. sternohyoidei and omohyoidei, which lower the floor of the oral cavity. Myers *et al.* (2004:22 concluded "...that all microhylids [including *Callulina kreffti*, *Dermatonotus*, *Dyscophus guineti*, *Gastrophryne carolinensis*, *G. olivacea*, and *Hypopachus variolosus*, *Kaloula pulchra*, *Microhyala achatina*, *M. pulchra*, *Phrynomantis bifasciatus*, *P. microps*, *Platypelis tuberifera*, *Scaphiophryne calcarata*, *S. gottlebei*, *S. marmorata*, and *S. pustulosa* in their study] are capable of lateral tongue movements and that they share a muscular hydrostatic mechanism of tongue protraction with *Hemissus*." This allows these frogs to direct the tongue laterally as well as anteriorly, and in elevation relative to the head. In the same paper (p. 29), these authors pointed out "...that the complex anatomy of the m. intermandibularis and unusually shaped mentomeckelian bones in microhylids are not functionally related to the ability to protract the tongue laterally." Nonetheless, these peculiar modifications of the mandible are associated with protraction of the hyoid, an action that facilitates extension of the m. hyoglossi as the tongue is protracted. Retraction of the hyoid is powered by the mm. sternohyoidei and omohyoidei as the m. hyoglossi retract the tongue. Because this mandibular morphology seems to be ubiquitous in the Gastrophryninae and Phrynomerinae, it seems somehow inextricably linked with this novel mechanism of tongue protrusion and feeding and deserves further study.

Like members of Gastrophryninae, *Phrynomantis bifasciatus* has a robust hyoid with posteromedial processes that are expanded

posteriorly. A thick cartilaginous ridge at the posterior border of the hyoid corpus separates the heads of the posteromedial processes (de Villiers 1930). The tongue is retracted by the mm. hyoglossi, which originate from the posterior part of the posteromedial processes. From their origin, this pair of muscles course anteriorly over the ventral surface of the hyoid corpus and then reverse direction by wrapping up and over the anterior margin of the hyoid plate to run posteriorly and insert on the ventral surface of the tongue pad. In addition, the m. geniohyoideus medialis inserts on the expanded posteromedial processes.

*Osteological trends in Gastrophryninae.*—The most obvious suites of changes in this clade involve the cranium and the pectoral girdle. In nearly all gastrophrynines with the exception of *Stereocyclops*, the angles of the jaw lie forward relative to the otic capsules. This anterior shift in the position of the jaw has some interesting cranial corollaries. The planum antorbitale is oriented anterolaterally instead of laterally. The basal process is elaborated as a robust block of cartilage bracing the pterygoid against the anterolateral corner/margin of the otic capsule. The medial ramus of the pterygoid is exceedingly short. The anterior shift of the jaws is correlated with snouts that protrude beyond the end of the mouth and the development of a medial prenasal process; the forward shift of the olfactory capsules is accommodated by the anteroventral deflection/rotation of the alary processes of the premaxillae. Doubtless these changes are associated with the functional need to maintain a wide gape for the unique mechanism of tongue protrusion. The trends are least evident in *Nelsonophryne* and *Melanophryne*, which have a basal position in Gastrophryninae (Figure 8). *Stereocyclops* seems atypical; however, the structure of its skull as depicted by Carvalho (1948:Fig.1) suggests that the posterior position of the jaw and the wide skull might have been derived from a more typical gastrophrynine because (1) the planum antorbitale has an anteromedial orientation and the medial ramus of the pterygoid is short.

Other significant trends in cranial evolution include narrowing of the cranium in most taxa, along with loss of the neopalatine and reduction of the vomer. In taxa lacking a neopalatine, the planum antorbitale may be mineralized and the ossification of the sphenethmoid may invade the medial part of the planum. In most gastrophrynines, the vomer is a small, crescent-shaped bone that supports the anterior and anteromedial margins of the choana; a short anterior process may be present. In *Adelastes*, a slender posterior process is present. A few possess a so-called divided vomer (e.g., *Arcovomer*, *Hamptophryne*, *Relictivomer*), in which there is a vestige of the posterior process of vomer in the region of the sphenethmoid.

The other architectural unit that is modified among gastrophrynines is the pectoral girdle. A transverse clavicle extending from the pars acromialis of the scapula to the medial portion of the girdle is present only in *Stereocyclops* and *Dermatonotus*; it is unclear whether the procoracoid cartilage is reduced in these taxa or not. In the remaining gastrophrynines the clavicle is either reduced or absent. When the clavicle is reduced, the procoracoid cartilage extends from the midline to approximately the midlength of the coracoid, rather than to the lateral end of this bone. Reduction of the procoracoid cartilage ranges from (1) incomplete laterally to (2) incomplete medially to (3) present laterally and medially, but absent at the mid-clavicle to (4) absence, but the latter only occurs in taxa lacking any vestige of a clavicle. Likewise, as mid-zonal components are lost, the anterior part of the epicoracoid cartilage diminishes in size; in its minimal configuration, it forms a low bridge uniting the anteromedial corners of the coracoids.

In contrast to the anterior zonal elements, the coracoids tend to be stout elements with expanded sternal ends. In taxa lacking clavicles and procoracoids, the anterior angle between the long axes of the coracoids tends to be more acute, such that the sternal end of the girdle seems to lie significantly more posterior in the abdomen.

Understanding the phylogenetic and functional significance of these morphological differences is the challenge facing anuran biologists and it is one that requires a great deal more investigation of the morphology, development, phylogeny, and behavior of microhylids. We have only begun to describe structural diversity of these anurans, which rivals the range of diversity observed in all other neobatrachians. Detailed and complete descriptions of larvae and adults need to be generated so that taxa can be compared. Intraspecific variation in speciose genera (e.g., *Chiasmocleis*, *Elachistocleis*) should be assessed. Sexual dimorphism in osteology is unknown and uninvestigated. Feeding behavior should be documented and detailed myological studies undertaken to understand the relationship among the structure of the mandible, the hyoid, and the pectoral girdle, and tongue protraction. And last, studies of the larvae and their development must be undertaken to understand the relationship between chondrocranial structure, the closure of the nares soon after hatching, chemoreception, respiration, and suspension feeding. Surely, the present work has created more questions than it has resolved.

### Acknowledgments

We thank William E. Duellman (Univ. Kansas) for comments on the manuscript, and Darrel Frost (American Museum of Natural History) and José Rosado (Museum of Comparative Zoology, Harvard University) for the loan of specimens. A National Science Foundation grant (EF 0334928 to L.T.) provided indispensable financial support for all three authors. 

### References

- Alberch, P. and E. Gale. 1985. A developmental analysis of an evolutionary trend: digital reduction in amphibians. *Evolution* 39: 8–23.
- AmphibiaWeb: Information on amphibian biology and conservation. [web application]. 2011. Berkeley, California: AmphibiaWeb. Available: <http://amphibiaweb.org/>.
- Cannatella, D. C. 1999. Architecture. Cranial and Axial Musculoskeleton. Pp. 52–91 in R. W. McDiarmid and R. Altig (eds.), *Tadpoles. The Biology of Anuran Larvae*. Chicago. University of Chicago Press. xiv + 444 pp.
- Carvalho, A. L. 1948. Sobre a validade de *Stereocyclops incrassatus* Cope, 1871 e *Hypopachus mülleri* (Boettger), 1885. *Boletim do Museu Nacional* 84: 1–14.
- Carvalho, A. L. 1954. A preliminary synopsis of the genera of American microhylid frogs. *Occasional Papers of the Museum of Zoology, University of Michigan* 555: 1–19.
- Darst C. R., and D. C. Cannatella. 2004. Novel relationships among hyloid frogs inferred from 12S and 16S mitochondrial DNA sequences. *Molecular Phylogenetics and Evolution* 31: 462–475.
- da Silva, H. R. and D. J. Meinhardt. 1999. The generic status of *Adelophryne tridactyla*: osteology, synonymy, and comments on the genus *Syncope*. *Journal of Herpetology* 33: 159–164.
- de Sá, R. O. and L. Trueb. 1991. Osteology, skeletal development, and chondrocranial structure of *Hamptophryne boliviana* (Anura: Microhylidae). *Journal of Morphology* 209: 311–330.
- Devanesan, D. 1922. Notes on the anatomy of *Cacopus systema*, an Indian toad of the family Engystomatidae. *Proceedings of the Zoological Society of London* 2: 527–556.
- de Villiers, C. G. S. 1930. On the cranial characters of the South African brevicipitid, *Phrynomerus bifasciatus*. *Quarterly Journal of Microscopical Science* 73: 667–705.
- de Villiers, C. G. S. 1934. Die Schädelanatomie der Rhombophryne testudo Boettger in bezug auf ihre Verwandtschaft mit den malagassischen Brevicipitiden. *Anatomischer Anzeiger* 78: 295–310.
- Dingerkus, G. and L. D. Uhler. 1977. Enzyme clearing of Alcian blue stained whole small vertebrates for demonstration of cartilage. *Stain Technology* 52: 229–232.
- Donnelly, M. A., R. O. de Sá, and C. Guyer. 1990. Description of the tadpoles of *Gastrophryne pictiventris* and *Nelsonophryne aterrima* (Anura: Microhylidae), with a review of morphological variation in free-swimming microhylid larvae. *American Museum Novitates* 2976: 1–19.
- Duellman W. E. and L. Trueb. 1994. *Biology of Amphibians*. Baltimore. Johns Hopkins University Press. 670 pp.
- Edgar, R. C. 2004. MUSCLE: multiple sequence alignment with high accuracy and high throughput. *Nucleic Acids Research* 32: 1792–1797.
- Emerson, S. B. 1976. A preliminary report on the superficial throat musculature of the Microhylidae and its possible role in tongue action. *Copeia* 1976: 546–551.

- Fabrezi, M. and P. Alberch. 1996. The carpal elements of Anura. *Herpetologica* 52: 188–204.
- Frost, D. R. 2011. Amphibian Species of the World: an online reference. Version 5.5 (31 January, 2011). Electronic Database accessible at <http://research.amnh.org/vz/herpetology/amphibia/> American Museum of Natural History, New York, USA.
- Frost, D. R., T. Grant, J. Faivovich, R. H. Bain, A. Haas, C. F. B. Haddad, R. O. de Sá, A. Channing, M. Wilkinson, S. C. Donnellan, C. Raxworthy, J. A. Campbell, B. L. Blotto, P. Moler, R. C. Drewes, R. A. Nussbaum, J. D. Lynch, D. M. Green, W. C. Wheeler. 2006. The amphibian tree of life. *Bulletin of the American Museum of Natural History* 297: 1–370.
- Gosner, K. L. 1960. A simplified table for staging anuran embryos and larvae with notes on identification. *Herpetologica* 16: 183–190.
- Greenbaum, E. 2006. Molecular systematics of New World microhylid frogs, with an emphasis on the Middle American genus *Hypopachus*. Unpublished Ph.D. Thesis, University of Kansas.
- Haas, A. 2001. Mandibular arch musculature of anuran tadpoles, with comments on homologies of amphibian jaw muscles. *Journal of Morphology* 247: 1–33.
- Haas, A. 2003. Phylogeny of frogs as inferred from primarily larval characters (Amphibia: Anura). *Cladistics* 19: 23–89.
- Jurgens, J. D. 1971. The morphology of the nasal region of Amphibia and its bearing on the phylogeny of the group. *Annale Universiteit van Stellenbosch* 46 (Series A): 1–146.
- Klymkowsky, M.W. and J. Hanken. 1991. Whole-mount staining of *Xenopus* and other vertebrates. Pp. 419–441 in B. K. Kay and H. B. Peng (eds.), *Xenopus laevis: Practical Uses in Cell and Molecular Biology. Methods in Cell Biology* 36. New York. Academic Press.
- Langone, J. A., E. O. Lavilla, D. D. Echeverría, S. Mangione, and M. V. Segalla. 2007. Morfología externa e interna de la larva de *Chiasmocleis leucosticta* (Boulenger, 1888) (Amphibia, Anura, Microhylidae). *Publicacion Extra, Museo Nacional de Historia Natural y Antropología (Montevideo)* 2: 1–25.
- Larson, P. M. 2002. Chondrocranial development in larval *Rana sylvatica* (Anura: Ranidae): morphometric analysis of cranial allometry and ontogenetic shape change. *Journal of Morphology* 252: 131–144.
- Larson, P. M. 2004. Chondrocranial morphology and ontogenetic allometry in larval *Bufo americanus* (Anura, Bufonidae). *Zoomorphology* 123: 95–106.
- Lavilla, E. O. 1992. The tadpole of *Dermatonotus muelleri* (Anura: Microhylidae). *Bollettino Museo regionale di Scienze naturali (Torino)* 10: 63–71.
- Lavilla, E. O. and J. A. Langone. 1995. Estructura del condrocraneo y esqueleto visceral de larvas de *Elachistocleis bicolor* (Valenciennes, 1838) (Anura: Microhylidae). *Cuadernos de Herpetología* 9: 45–49.
- Lavilla, E. O., M. Vaira, and L. Ferrari. 2003. A new species of *Elachistocleis* (Anura: Microhylidae) from the Andean yungas of Argentina, with comments on the *Elachistocleis ovalis* – *E. bicolor* controversy. *Amphibia-Reptilia* 24: 269–284.
- Lehr, E. and L. Trueb. 2007. Diversity among New World microhylid frogs (Anura: Microhylidae): morphological and osteological comparisons between *Nelsonophryne* (Günther 1901) and a new genus from Peru. *Zoological Journal of the Linnean Society* 149: 583–609.
- Meyers, J. J., J. C. O'Reilly, J. A. Monroy, and K. C. Nishikawa. 2004. Mechanism of tongue protraction in microhylid frogs. *Journal of Experimental Biology* 207: 21–31.
- Noble, G. K. and H. W. Parker. 1926. A synopsis of the brevipitid toads of Madagascar. *American Museum Novitates* 232: 1–21.
- Parker, W. H. 1934. *A Monograph of the Frogs of the Family Microhylidae*. London. British Museum (Natural History). 208 pp.
- Parker, W. K. 1881. On the structure and development of the skull in the Batrachia. Part III. *Philosophical Transactions of the Royal Society of London* 172: 1–266.
- Posada, D. 2008. jModelTest: phylogenetic model averaging. *Molecular Biology and Evolution* 25: 1253–1256.
- Pugener, L.A., A. M. Maglia, and L. Trueb. 2003. Revisiting the contribution of larval characters to an analysis of phylogenetic relationships of basal anurans. *Zoological Journal of the Linnean Society* 139: 129–155.
- Ramaswami, L. S. 1932a. The cranial anatomy of *Glyphoglossus molussus* (Gunther). *The Half-yearly Journal of the Mysore University* 6: 1–12.
- Ramaswami, L. S. 1932b. The cranial osteology of the south Indian Engystomatidae (Anura). *The Half-yearly Journal of the Mysore University* 6: 32–44.
- Ramaswami, L. S. 1940. Some aspects of the chondrocranium in the tadpoles of South Indian frogs. *Journal of the Mysore University* 1: 15–41.
- Roelants, K., D. J. Gower, M. Wilkinson, S. P. Loader, S. D. Biju, K. Guillaume, L. Moriau, F. Bossuyt. 2007. Global patterns of diversification in the history of modern amphibians. *Proceedings of the National Academy of Sciences USA* 104: 887–892.

- Thompson, J. D., T. J. Gibson, F. Plewniak, F. Jeanmougin, D. G. Higgins. 1997. The ClustalX windows interface: flexible strategies for multiple sequence alignment aided by quality analysis tools. *Nucleic Acids Research* 24: 4876–4882.
- Van Bocxlaer, I., K. Roelants, S. D. Biju, J. Nagaraju, F. Bossuyt. 2006. Late Cretaceous vicariance in Gondwanan amphibians. *PLoS ONE* 1: e74.
- van der Meijden, A., M. Vences, A. Meyer. 2004. Novel phylogenetic relationships of the enigmatic brevipitine and scaphiophryne toads as revealed by sequences from the nuclear *Rag-1* gene. *Proceedings of the Royal Society of London (Suppl.)* 271: S378–S381.
- van der Meijden, A., M. Vences, S. Hoegg, R. Boistel, A. Channing, A. Meyer. 2007. Nuclear gene phylogeny of narrow-mouthed toads (Family: Microhylidae) and a discussion of competing hypotheses concerning their biogeographic origins. *Molecular Phylogenetics and Evolution* 44: 1017–1030.
- Vera Candiotti, M. F. 2006. Morfología larval de *Chiasmocleis panamensis*, con comentarios sobre la variabilidad morfológica interna en renacuajos de Microhylidae (Anura). *Alytes* 24: 91–108.
- Vera Candiotti, M. F. 2007. Anatomy of anuran tadpoles from lentic water bodies: systematic relevance and correlation with feeding habits. *Zootaxa* 1600: 1–175.
- Walker, C. F. 1973. A new genus and species of microhylid frog from Ecuador. *Occasional Papers of the Museum of Natural History, University of Kansas* 20: 1–7.
- Walker, C. F. and W. E. Duellman. 1974. Description of a new species of microhylid frog, *Chiasmocleis*, from Ecuador. *Occasional Papers of the Museum of Natural History, University of Kansas* 26: 1–6.
- Wassersug, R. J. and W. F. Pyburn. 1987. The biology of the Pe-ret' Toad, *Otophryne robusta* (Microhylidae), with special consideration of its fossorial larva and systematic relationships. *Zoological Journal of the Linnean Society* 91: 137–169.
- Wells, K. D. 2007. *The Ecology and Behavior of Amphibians*. The University of Chicago Press. 1400 pp.
- Wild, E. R. 1995. New genus and species of Amazonian microhylid frog with a phylogenetic analysis of new world genera. *Copeia* 1995: 837–849.
- Wollenberg, K. C., D. R. Vietes, A. van der Meijden, F. Glaw, D. C. Cannatella, and M. Vences. 2008. Patterns of endemism and species richness in Malagasy frogs support a key role of mountainous areas for speciation. *Evolution* 62: 1890–1907.
- Wu, S.-H. 1994. Phylogenetic relationships, higher classification, and historical biogeography of the microhylid frogs (Lissamphibia: Anura: Brevicipitidae and Microhylidae). Unpublished Ph.D. Thesis, University of Michigan, Ann Arbor.
- Zweifel, R. G. 1962. Results of the Archbold Expeditions. No. 83. Frogs of the microhylid genus *Cophixalus* from the mountains of New Guinea. *American Museum Novitates* 2087: 1–16.
- Zweifel, R. G. 1971. Results of the Archbold Expeditions. No. 96. Relationships and distribution of *Genyophryne thomsoni*, a microhylid frog of New Guinea. *American Museum Novitates* 2469: 1–13.
- Zweifel, R. G. 1972. Results of the Archbold Expeditions. No. 97. A revision of the frogs of the subfamily Asterophryinae Family Microhylidae. *Bulletin of the American Museum of Natural History* 148: 413–546.
- Zweifel, R. G. 1985. Australian frogs of the family Microhylidae. *Bulletin of the American Museum of Natural History* 182: 266–388.
- Zweifel, R. G. 1986. A new genus and species of microhylid frog from the Cerro de la Neblina Region of Venezuela and a discussion of relationships among New World microhylid genera. *American Museum Novitates* 2863: 1–24.
- Zweifel, R. G. 2000. Partition of the Australopapuan microhylid frog genus *Sphenophryne* with descriptions of new species. *Bulletin of the American Museum of Natural History* 253: 1–130.
- Zweifel, R. G. and A. Allison. 1982. A new montane microhylid frog from Papua New Guinea, and comments on the status of the genus *Aphantophryne*. *American Museum Novitates* 2723: 1–14.
- Zweifel, R. G. and F. Parker. 1989. New species of microhylid frogs from the Owen Stanley Mountains of Papua New Guinea and resurrection of the genus *Aphantophryne*. *American Museum Novitates* 2954: 1–20.
- Zwickl, D. J. 2006. Genetic algorithm approaches for the phylogenetic analysis of large biological sequence datasets under the maximum likelihood criterion. Unpublished Ph.D. Thesis, University of Texas, Austin, USA.

**Appendix I.** Cleared-and-stained specimens examined. All are from the collections of the University of Kansas Biodiversity Institute (KU) or the American Museum of Natural History.

*Adelastes hylonomos*. VENEZUELA: AMAZONAS FEDERAL TER: DEPARTAMENTO RÍO NEGRO: vicinity of Neblina Base Camp on Río Baria, 140 m, AMNH A123697.

*Arcovomer passarellii*. BRAZIL: RIO DE JANEIRO: Itaguaí, KU 93237.

*Chiasmocleis anaitipes*. ECUADOR: SUCUMBÍOS: Santa Cecilia, 340 m, KU 146036 (paratype).

*Ctenophryne geayi*. VENEZUELA: BOLÍVAR: 13 km S, 1 km E Puente Cuyuni, KU 167777.

*Elachistocleis cesarii*. BRAZIL: SÃO PAULO: São Paulo, Campo Grande, Santo Andre, KU 93246.

*Elachistocleis* sp. VENEZUELA: BOLÍVAR: El Dorado–Santa Elena de Uairen Rd, Km 144, 1210 m, KU 167780, male, 44.0 mm SVL.

*Gastrophryne carolinensis*. **Larvae:** USA: FLORIDA: Dade Co.: Larvae collected and reared in the laboratory by W. Meshaka in 1991: KU 222712–14 (Stage 26), KU 222715 (Stage 27), KU 222716 (Stage 28), KU 222717 (Stage 29), KU 222718 (Stage 30), KU 222719–22 (Stage 31), KU 222723 (Stage 36), KU 222724–26 (Stage 41), KU 222727–28 (Stage 43), KU 222729–32 (Stage 42), KU 222733–35 (Stage 44), KU 222736–39 (Stage 45), KU 222740–42 (Stage 46); larvae collected by D. Paulson: KU 297605 (Stages 33, 34, 37, 38). **Adults:** USA: FLORIDA: Alachua Co.: near Hawthorne, KU 297366–68; Broward Co.: Hollywood, 7<sup>th</sup> Avenue, KU 297378; Dade Co.: Florida City, KU 297371; Marion Co.: 10 mi E Silver Springs, KU 60204; Silver Springs, KU 90966.

*Hamptophryne boliviana*. ECUADOR: SUCUMBÍOS: Santa Cecilia, 340 m, KU 124129 (larva), 153007.

*Hypopachus variolosus*. MEXICO: CHIAPAS: 14.4 km SW Las Cruces, 700 m, KU 68645.

*Myersiella microps*. BRAZIL: RIO DE JANEIRO: Terezopolis, KU 93264, male.

*Syncope antenori*. ECUADOR: SUCUMBÍOS: Puerto Libre, Río Aguarico, 570 m, KU 124003 (paratype).

**Appendix II.** GenBank accession numbers for DNA sequences of loci used in the phylogenetic analysis.

Taxon	Family	16S (mt)	RAG-1 (nuc)	RAG-2 (nuc)	TYR (nuc)
<i>Arthroleptis variabilis</i>	Arthroleptidae	AY322301	AY571642	EF396112	AY341756
<i>Breviceps fuscus</i>	Brevicipitidae	AF215365	AY571644	DQ019520	EF395962
<i>Hemisis marmoratus</i>	Hemisotidae	DQ283430	—	EF396127	EF395975
<i>Kassina maculata</i>	Hyperoliidae	AF215444	AY571651	—	—
<i>Anodonthyla boulengerii</i>	Microhylidae	EU341091	EF396072	EF396110	EF395959
<i>Aphantophryne pansa</i>	Microhylidae	DQ283195	—	—	—
<i>Asterophrys turpicola</i>	Microhylidae	—	—	—	EF395961
<i>Barygenys flavigularis</i>	Microhylidae	AY948767	AY948943	—	—
<i>Calluella guttulata</i>	Microhylidae	DQ283144	EF396078	EF396115	EF395964
<i>Chaperina fusca</i>	Microhylidae	DQ283145	-	-	DQ282938
<i>Chiasmocleis hudsoni</i>	Microhylidae	EU201099	EF396079	EF396118	EF395967
<i>Chiasmocleis shudikarensis</i>	Microhylidae	—	EF396080	EF396117	EF395966
<i>Choerophryne</i> sp.	Microhylidae	DQ283207	—	—	—
<i>Cophixalus</i> "sp. A"	Microhylidae	DQ347334	DQ347276	—	DQ347183
<i>Cophyla phyllodactyla</i>	Microhylidae	EU341112	EU341122	—	—
<i>Copiula</i> sp.	Microhylidae	DQ283208	—	—	—
<i>Ctenophryne geayi</i>	Microhylidae	DQ283383	—	—	DQ282993
<i>Dasypops schirchi</i>	Microhylidae	DQ283095	—	—	DQ282922
<i>Dermatonotus muelleri</i>	Microhylidae	DQ283330	EF396082	EF396120	EF395969

## Appendix II. Continued.

Taxon	Family	16S (mt)	RAG-1 (nuc)	RAG-2 (nuc)	TYR (nuc)
<i>Dyscophus antongilii</i>	Microhylidae	EU341120	AY571648	DQ019525	EF395970
<i>Dyscophus insularis</i>	Microhylidae	EU341119	EF396083	EF396121	EF395971
<i>Elachistocleis ovalis</i>	Microhylidae	DQ283405	EF396085	EF396123	EF395972
<i>Gastrophryne carolinensis</i>	Microhylidae	X86278	EF396086	EF396124	EF395973
<i>Gastrophryne olivacea</i>	Microhylidae	DQ283268	DQ347280	—	DQ347188
<i>Genyophryne thomsoni</i>	Microhylidae	DQ283209	—	—	—
<i>Glyphoglossus molossus</i>	Microhylidae	AB201193	EF396087	EF396125	EF395974
<i>Hamptophryne boliviana</i>	Microhylidae	DQ283438	EF396088	EF396126	—
<i>Hoplophryne rogersi</i>	Microhylidae	DQ283419	EF396089	EF396128	EF395976
<i>Hylophorbus rufescens</i>	Microhylidae	EF017958	EF018047	—	—
<i>Hypopachus variolosus</i>	Microhylidae	—	EF396090	EF396129	EF3959771
<i>Kalophrynus pleurostigma</i>	Microhylidae	DQ283146	AY948919	—	—
<i>Kaloula pulchra</i>	Microhylidae	DQ283398	EF396091	EF396130	EF395978
<i>Kaloula taprobanica</i>	Microhylidae	AF249057	AY948915	—	AF249163
<i>Liophryne rhododactyla</i>	Microhylidae	DQ283199	—	—	—
<i>Melanobatrachus indicus</i>	Microhylidae	EF017964	EF018053	—	—
<i>Metaphrynella sundana</i>	Microhylidae	EF017954	EF018043	—	—
<i>Microhyla heymonsi</i>	Microhylidae	DQ283382	EF396095	EF396133	EF395979
<i>Micryletta inornata</i>	Microhylidae	AF285207	EF396096	EF396135	EF395981
<i>Nelsonophryne aequatorialis</i>	Microhylidae	AY326067	—	—	—
<i>Oreophryne</i> sp.	Microhylidae	EF017957	EF018046	—	—
<i>Otophryne pyburni</i>	Microhylidae	—	EF396097	EF396136	EF395982
<i>Paradoxophyla palmata</i>	Microhylidae	EU341121	EF396098	EF396137	EF395983
<i>Phrynomantis annectens</i>	Microhylidae	AF215377	AY57165	EF396139	EF395985
<i>Phrynomantis bifasciatus</i>	Microhylidae	DQ283154	EF396100	EF396138	EF395984
<i>Platypelis grandis</i>	Microhylidae	DQ283410	EF396101	EF396140	EF395986
<i>Plethodontohyla brevipes</i>	Microhylidae	—	EF396103	EF396142	EF395987
<i>Ramanella</i> cf. <i>obscura</i>	Microhylidae	AF215382	EF396104	EF396143	EF395989
<i>Rhombophryne testudo</i>	Microhylidae	EU341110	EF396105	EF396144	EF395990
<i>Scaphiophryne calcarata</i>	Microhylidae	AY834193	EF396106	DQ019548	EF395991
<i>Sphenophryne cornuta</i>	Microhylidae	AY948766	AY948942	-	-
<i>Stumpffia pygmaea</i>	Microhylidae	EU341065	EF396108	EF396146	EF395992
<i>Synapturanus mirandaribeiroi</i>	Microhylidae	—	—	—	DQ282908
<i>Synapturanus</i> sp.	Microhylidae	EF017962	EF018051	—	—
<i>Uperodon systoma</i>	Microhylidae	EF017960	EF018049	—	—
<i>Xenobatrachus obesus</i>	Microhylidae	EF017959	EF018048	—	—
<i>Pyxicephalus adspersus</i>	Pyxicephalidae	AF215505	DQ019508	DQ019543	DQ347146

**Appendix III.** Table of osteological characters. + = condition present; - = character absent; ? in gray bar = condition unknown; ? in white cell = condition could not be determined from specimen; F = fused; D = divided; S = spur of bone; M = mineralized, but not endochondral bone; V = vestigial; NA = not applicable.

	<i>Adelastes hylonomos</i>	<i>Altigius alios</i>	<i>Arcovomer passarellii</i>	<i>Chiasmocleis albopunctata</i>	<i>Chiasmocleis anaptipes</i>	<i>Ctenophryne geayi</i>	<i>Dasydops schirchi</i>	<i>Dermatonothus muelleri</i>	<i>Elachistocleis cesarii</i>	<i>Elachistocleis skotogaster</i>	<i>Gastrophryne carolinensis</i>	<i>Hamptophryne boliviana</i>	<i>Hypopachus variolosus</i>	<i>Hyophryne histrio</i>	<i>Melanophryne barbatula</i>	<i>Melanophryne caipish</i>	<i>Myersiella subnigra</i>	<i>Nelsonophryne aequatorialis</i>	<i>Nelsonophryne aterrima</i>	<i>Relictivomer pearsei</i>	<i>Stereoclyps incrassatus</i>	<i>Synapturanus mirandaribeiroi</i>	<i>Syncope antenori</i>	<i>Syncope tridactyla</i>	
<b>Characters</b>	<b>1</b>	<b>2</b>	<b>3</b>	<b>4</b>	<b>5</b>	<b>6</b>	<b>7</b>	<b>8</b>	<b>9</b>	<b>10</b>	<b>11</b>	<b>12</b>	<b>13</b>	<b>14</b>	<b>15</b>	<b>16</b>	<b>17</b>	<b>18</b>	<b>19</b>	<b>20</b>	<b>21</b>	<b>22</b>	<b>23</b>	<b>24</b>	
Skull proportions				?			?																		
Broader than long	-	-	+	-	+		+	-	-	-	+	+	+	+	+	-	+	+		+		-	-		
Width $\cong$ length	+	+	-	+	-		-	-	-	-	-	-	-	-	-	-	-	-	-		-		+	+	
Width < length	-	-	-	-	-		-	+	+	+	-	-	-	-	-	+	-	-		-		-	-		
Angle of jaw: position				?			?							?						?				?	
Posterior, near posterior part of otic capsule or beyond	-	-	-	-	-		-	-	-	-	-	-	-		-	-	-	-	-		+	-	-		
At $\pm$ mid-level otic capsule	-	-	-	-	-		-	-	-	-	+	-		+	+	-	-	-	-		-	-	-		
Anterior to otic capsule or near anterior level of capsule	+	+	+	+	+		+	+	+	+	-	+		-	-	+	+	+	+		-	+	+		
Pterygoid		?		?			?							?						?					
Medial ramus reduced/absent	+		+		-	-	+	+	+	+	+	+	+		-	-	+	-	-		-	+	+	-	
Anterior ramus elaborated	-		-		-	-	-	-	-	-	-	-			-	-	-	-	-		+	-	-	-	
Maxillary arcade																									
Maxilla-quadratojugal articulation present	-	-	-	-	-	+	-	+	-	-	+	+	+	+	+	+	-	+	-	-	+	-	-	-	
Dentition present	-	-	-	-	-	-	-	-	-	-	-	-	-	-	-	-	-	-	-	-	-	-	-	-	
Quadratojugal																									
Present	+	+	+	+	+	+	+	+	S	+	+	+	+	+	+	+	+	+	+	+	+	+	-	-	
Snout							?							?						?					
Protuberant: premaxilla deflected anteriorly/ventrally	+	+	+	+	+	+		+	+	+	+	+	+		-	-	+	-	-		-	+	+	?	
Sphenethmoid		?					?																		
Divided	?		+	+	+	+		+	+	+	+	+	+	+	+	+	+	+	+	+	+	+	?	+	+
No division evident: M	+		-	-	-	-		-	-	-	-	-	-	-	-	-	-	-	-	-	-	+	-	-	
Mandible		?		?	?		?													?	?	?		?	
Syndesmotoc symphysis absent	+		+			+		+	+	+	+	+	+	+	+	+	+	+	+				+		
Mentomeckelian diverticulum present	+		+			+		+	+	+	+	+	+	+	+	+	+	+	+				+		
Nasals		?		?			?							?						?	?	?		?	
Large, covering all or most of nasal capsule	+		+		+	+		+	+	+	+	+	+		-	-	+	-	-				+		
Moderate to small; large parts of nasal capsule exposed	-		-		-	-		-	-	-	-	-	-		+	+	-	+	+				-		

Appendix III. *Continued.*

Characters	1	2	3	4	5	6	7	8	9	10	11	12	13	14	15	16	17	18	19	20	21	22	23	24
Neopalatine		?					?							?						?				?
Present as independent element	-		+	-	-	-		-	-	-	-	+	-		+	+	-	+	+		-	-	-	
Present, fused to vomer	-		-	-	-	-		-	-	-	-	-	-		-	-	-	-	-		+	?	-	-
Present fused to sphenethmoid	-		-	-	-	-		-	-	-	-	-	-		-	-	-	-	-		-	-	-	
Absent	+		-	+	+	+		+	+	+	+	-	+		-	-	+	-	-		-	+	?	+
Vomer							?							?										?
Single, whole: choanal and posterior parts	+	?	-	-	-	-		-	-	-	-	-	-		-	-	-	-	-		-	-	-	
Single: only choanal part	+	?	?	-	+	+	+	+	+	+	+	-	+		+	+	+	+	+		-	+	-	+
Divided	-	-	+	-	-	-		-	-	-	-	+	-		-	-	-	-	-		+	-	-	-
Vomer fused to sphenethmoid	?	-	-	-	-	-		-	-	-	-	-	-		-	-	-	-	-		-	-	+	?
Posterior vomer fused with neopalatine	-	-	-	-	-	-		-	-	-	-	-	-		-	-	-	-	-		-	-	-	+
Stapes		?		?			?							?						?		?		
Present	+		-		+	+		+	+	+	+	+	+		-	-	+	+	+		+		+	+
Hyoid		?	?		?	?	?							?						?	?	?		
Parahyoid bone	+			-				M	-	-	-	-	-		-	-	-	-	-				-	-
Slit	-			+				+	?	-	+	+	?		-	-	?	-	-				?	+
Ventral protuberance	-			+				-	-	+	-	-	-		-	+	?	+	+				-	-
Axial Column				?			?							?									?	
8 presacrals	+	+	+		+	+		+	+	+	+	+	+		+	-	+	+	+	+	+	+	-	-
7 presacrals	-	-	-		-	-		-	-	-	-	-	-		-	+	-	-	-	-	-	-	-	-
6 presacrals	-	-	-		-	-		-	-	-	-	-	-		-	-	-	-	-	-	-	-	+	+
Presacrals I and II fused	-	-	-		-	-		-	-	-	-	-	-		-	+	-	-	-	-	-	-	+	+
Sacrum composed of 2 vertebrae	-	-	-		-	-		-	-	-	-	-	-		-	-	-	-	-	-	-	-	+	+
Last presacral amphicoelous	+	-	+		-	+		+	+	-	+	+	+		-	+	-	+	+	+	+	-	-	-
Vestigial transverse processes on urostyle	-	-	-		-	-		-	-	-	-	-	-		-	-	+	-	-	-	-	-	+	+
Clavicle																							?	
Present, complete	-	-	-	-	-	-	-	+	-	-	-	-	+		-	-	-	-	-	-	-	+	-	-
Present right, reduced	-	-	+	-	-	-	+	-	+	-	-	+	-	+	-	-	-	-	-	-	-	-	+	+
Present left, reduced	-	+	-	+	+	-	-	-	-	-	-	-	-	-	-	-	-	-	-	-	+	-	-	-
Present middle, reduced	-	-	-	-	-	-	-	-	-	+	-	-	-	-	+	+	-	-	-	-	-	-	-	-
Absent	+	-	-	-	+	+	-	-	-	+	-	-	-	-	-	-	+	+	+	+	-	-	-	-
Coracoid		?		?																?				?
Fused to scapula	+		-		-	+	-	M	-	-	+	-	-	-	-	-	-	-	-	-	-	-	+	
Procoracoid cartilage		?																		?		?		
To lateral coracoid	-		-	-	-	-	-	-	-	-	-	-	-	+	-	-	-	-	-	-	-	-	-	-
To mid-coracoid or medial	-		+	+	+	-	-	+	-	-	+	-	+	-	+	-	-	-	-	-	-	-	+	+
Present, incomplete medially	-		-	-	-	-	-	+	+	-	+	-	-	-	+	-	-	-	-	-	-	-	+	+
Present, incomplete laterally	-		-	-	+	-	-	+	+	-	-	-	+	-	-	-	-	-	-	+	-	-	-	-
Present, incomplete in the middle	-		+	-	-	-	-	+	+	+	-	+	+	-	-	-	-	-	-	-	-	-	-	-
Absent	+		-	-	-	+	+	-	-	-	+	-	-	-	-	-	+	+	+	+	?	-	-	-

**Appendix III.** *Continued.*

Characters	1	2	3	4	5	6	7	8	9	10	11	12	13	14	15	16	17	18	19	20	21	22	23	24
Epicoracoid cartilage		?															?			?	?			
Pointed bridge anterior to coracoids	-		-	-	-	-	-	-	-	-	+	-	-	-	-	-		+	+		-		-	-
Blunt union of coracoids, nothing or small point anterior	+		-	+	+	-	-	-	-	-	-	-	-	-	-	+		-	-		-		-	+
Blunt fusion united to procoracoid cartilages	-		+	-	-	-	-	-	+	±	-	-	+	+	-	-		-	+		-		+	+
Paired or fused independent elements	-		-	-	-	-	F	F	F/D	-	-	P	-	-	-	-		-	-		F		-	-
Independent of coracoid, each other and fused to proc	-		-	+	-	+	-	-	-	-	-	-	-	-	-	-		-	-		-		-	-
Absent, anterior to coracoids	-		-	-	-	-	-	-	-	-	+	-	-	-	-	-		-	-		-		-	+
Manus							?							?						?	?	?		
Digit II reduced	-	-	-	-	-	-		-	-	-	-	-	-		-	-	-	-	-				-	+
Digit III reduced	-	-	-	-	-	-		-	-	-	-	-	-		-	-	-	-	-				-	+
Digit V reduced	-	-	-	-	-	-		-	-	-	-	-	-		-	-	-	-	-				-	+
Terminal phalange not or only slightly differentiated	-	-	-	-	-	-		-	-	-	-	-	-		-	-	-	-	+			+	-	+
Terminal phalange narrow and rounded	+	-	-	-	-	-		-	-	-	-	-	-		-	-	-	-	-				-	-
Terminal phalange slightly bulbous	-	-	-	-	-	+		+	+	-	-	-	+		-	-	+	-	-				-	-
Terminal phalange slightly bilobed	-	+	-	-	+	-		-	-	-	-	+	-		+	+	-	+	-				+	-
Terminal phalange T-shaped	-	-	+	-	-	-		-	-	-	-	-	-		-	-	-	-	-				-	-
Phalangeal formula: 1-1-3-1	-	-	-	-	-	-		-	-	-	-	-	-		-	-	-	-	-				-	+
Phalangeal formula: 2-2-3-3	+	+	+	-	+	+		+	-	-	-	-	+		+	+	+	+	+				+	-
Distal Carpals 3-5 fused	+	?	+	?	+	+		+	+	+	+	+	+	?	+	+	+	-	-				+	+
Distal Carpals 4 and 5 fused	-	?	-	?	-	-		-	-	-	-	-	-	?	-	-	-	+	+				-	-
Pes				?			?							?						?	?	?		
Phalangeal formula: 2-2-3-4-3	+	+	+		+	+		+	+	+	+	+	+		+	+	+	+	+				-	-
Phalangeal formula: 1-2-3-4-3	-	-	-		-	-		-	-	-	-	-	-		-	-	-	-	-				+	-
Phalangeal formula: 1-2-3-4-2	-	-	-		-	-		-	-	-	-	-	-		-	-	-	-	-				-	+